NASA/TM–2015-104606 / Vol. 42

Technical Report Series on Global Modeling and Data Assimilation, Volume 42

Randal D. Koster, Editor

Soil Moisture Active Passive (SMAP) Project Calibration and Validation for the L4_C Beta-Release Data Product

John S. Kimball, Lucas A. Jones,Joseph Glassy, E. Natasha Stavros, Nima Madani, Rolf H. Reichle, Thomas Jackson, and Andreas Colliander

National Aeronautics and
Space Administration

Goddard Space Flight Center
Greenbelt, Maryland 20771

November 2015

NASA STI Program ... in Profile

Since its founding, NASA has been dedicated to the advancement of aeronautics and space science. The NASA scientific and technical information (STI) program plays a key part in helping NASA maintain this important role.

The NASA STI program operates under the auspices of the Agency Chief Information Officer. It collects, organizes, provides for archiving, and disseminates NASA's STI. The NASA STI program provides access to the NASA Aeronautics and Space Database and its public interface, the NASA Technical Report Server, thus providing one of the largest collections of aeronautical and space science STI in the world. Results are published in both non-NASA channels and by NASA in the NASA STI Report Series, which includes the following report types:

- TECHNICAL PUBLICATION. Reports of completed research or a major significant phase of research that present the results of NASA Programs and include extensive data or theoretical analysis. Includes compilations of significant scientific and technical data and information deemed to be of continuing reference value. NASA counterpart of peer-reviewed formal professional papers but has less stringent limitations on manuscript length and extent of graphic presentations.
- TECHNICAL MEMORANDUM. Scientific and technical findings that are preliminary or of specialized interest, e.g., quick release reports, working papers, and bibliographies that contain minimal annotation. Does not contain extensive analysis.
- CONTRACTOR REPORT. Scientific and technical findings by NASA-sponsored contractors and grantees.
- CONFERENCE PUBLICATION. Collected papers from scientific and technical conferences, symposia, seminars, or other meetings sponsored or co-sponsored by NASA.
- SPECIAL PUBLICATION. Scientific, technical, or historical information from NASA programs, projects, and missions, often concerned with subjects having substantial public interest.
- TECHNICAL TRANSLATION. English-language translations of foreign scientific and technical material pertinent to NASA's mission.

Specialized services also include organizing and publishing research results, distributing specialized research announcements and feeds, providing help desk and personal search support, and enabling data exchange services. For more information about the NASA STI program, see the following:

- Access the NASA STI program home page at http://www.sti.nasa.gov
- E-mail your question via the Internet to help@sti.nasa.gov
- Fax your question to the NASA STI Help Desk at 443-757-5803
- Phone the NASA STI Help Desk at 443-757-5802

NASA/TM–2015-104606/Vol. 42

Technical Report Series on Global Modeling and Data Assimilation,
Volume 42

Randal D. Koster, Editor

Soil Moisture Active Passive (SMAP) Project Calibration and Validation for the L4_C Beta-Release Data Product

John S. Kimball
University of Montana, Missoula, MT

Lucas A. Jones
University of Montana, Missoula, MT

Joseph Glassy
Lupine Logic, Inc., Missoula, MT

E. Natasha Stavros
Jet Propulsion Laboratory, Caltech, Pasadena, CA

Nima Madani
University of Montana, Missoula, MT

Rolf H. Reichle
NASA's Goddard Space Flight Center, Greenbelt, MD

Thomas Jackson
U.S. Department of Agriculture, Agricultural Research Service, Beltsville, MD

Andreas Colliander
Jet Propulsion Laboratory, Caltech, Pasadena, CA

National Aeronautics and
Space Administration

Goddard Space Flight Center
Greenbelt, Maryland 20771

November 2015

Level of Review: This material has been technically reviewed by technical management

TABLE OF CONTENTS

1 EXECUTIVE SUMMARY

During the post-launch Cal/Val Phase of SMAP there are two objectives for each science product team: 1) calibrate, verify, and improve the performance of the science algorithms, and 2) validate accuracies of the science data products as specified in the L1 science requirements according to the Cal/Val timeline. This report provides analysis and assessment of the SMAP Level 4 Carbon (L4_C) product specifically for the beta release. The beta-release version of the SMAP L4_C algorithms utilizes a terrestrial carbon flux model informed by SMAP soil moisture inputs along with optical remote sensing (e.g. MODIS) vegetation indices and other ancillary biophysical data to estimate global daily NEE and component carbon fluxes, particularly vegetation gross primary production (GPP) and ecosystem respiration (R_{eco}). Other L4_C product elements include surface (<10 cm depth) soil organic carbon (SOC) stocks and associated environmental constraints to these processes, including soil moisture and landscape FT controls on GPP and R_{eco} (Kimball et al. 2012). The L4_C product encapsulates SMAP carbon cycle science objectives by: 1) providing a direct link between terrestrial carbon fluxes and underlying freeze/thaw and soil moisture constraints to these processes, 2) documenting primary connections between terrestrial water, energy and carbon cycles, and 3) improving understanding of terrestrial carbon sink activity in northern ecosystems.

There are no L1 science requirements for the L4_C product; however self-imposed requirements have been established focusing on NEE as the primary product field for validation, and on demonstrating L4_C accuracy and success in meeting product science requirements (Jackson et al. 2012). The other L4_C product fields also have strong utility for carbon science applications; however, analysis of these other fields is considered secondary relative to primary validation activities focusing on NEE. The L4_C targeted accuracy requirements are to meet or exceed a mean unbiased accuracy (ubRMSE) for NEE of 1.6 g C m^{-2} d^{-1} or 30 g C m^{-2} yr^{-1}, emphasizing northern (≥45°N) boreal and arctic ecosystems; this is similar to the accuracy level of tower eddy covariance measurement-based observations (Baldocchi 2008).

Methods used for L4_C performance and validation assessments include: 1) qualitative evaluations of product fields in relation to characteristic spatial and seasonal patterns; 2) comparisons of daily carbon flux estimates with *in situ* tower eddy covariance measurement-based daily carbon (CO_2) flux observations from core tower validation sites [CVS]; 3) comparisons of daily carbon flux estimates with more extensive historical tower carbon flux observations from global FLUXNET data archives; and 4) consistency checks against other synergistic global carbon products, including soil carbon inventory records, satellite-based productivity (GPP) records, global GPP records derived from tower observation upscaling methods, and satellite-based observations of solar induced canopy fluorescence (SIF) as a surrogate for net photosynthesis and GPP. The above CVS comparisons involve approximately 30 individual tower sites; 12 of these sites emphasize northern (≥45°N) ecosystems, which are a primary focus of the L4_C product science objectives, while 18 sites represent a diverse range of other global biome types. The CVS comparisons involve active participation from SMAP tower validation partners who have agreed to contribute near real-time tower observation data records. A larger set of historical tower observation records from 228 globally distributed sites was also used for L4_C validation and was provided by the FLUXNET La Thuile tower data synthesis (Baldocchi 2008); these data extend over multiple (2-7) years and were used to establish climatological records for each site, including daily means and variability (standard deviation, SD). The above analyses exceed criteria established by the Committee on Earth Observing Satellites (CEOS) for Stage 1 validation, which supports beta release of the data based on a limited set of core validation sites. The above activities also satisfy criteria for Stage 2 validation by expanding to regional and global assessments that involve a diverse set of independent observations.

The primary methods and metrics used for the L4_C Cal/Val assessment include comparisons of collocated time series plots of tower observations with L4_C daily outputs. Comparisons involving CVS

sites are both spatially and temporally consistent, while comparisons using the more extensive FLUXNET tower site records are spatially but not temporally consistent as they involve product evaluations against historical tower observations. Other methods employed for L4_C evaluations include qualitative comparisons of latitudinal means and spatial distributions between L4_C outputs and similar spatially contiguous climatological variables derived from other independent satellite, inventory and model-based products. Metrics used to evaluate relative agreement between L4_C product fields and the independent observations include correlation (r-value), RMSE differences, bias and model sensitivity diagnostics. The metrics used to evaluate L4_C NEE correspondence and target accuracy requirements for product success primarily focus on bias-adjusted (primary) results, but also include secondary assessments of the unadjusted results.

This report notes several limitations in the beta-release version of the L4_C product, including the use of GEOS-5 surface temperatures rather than SMAP Radar-defined FT constraints to estimated carbon fluxes. These limitations will be addressed in the coming year prior to release of the validated data product. In addition, the validated product release will include more extensive validation activities involving a longer operational data record and associated calibration refinements; more detailed model sensitivity studies; and validation assessments using observational data records from several intensive field experiments. Despite these remaining areas, the beta-release L4_C product is of sufficient level of maturity and quality that it can be approved for distribution to and used by the larger science and application communities. This beta release also presents an opportunity to enable users to gain familiarity with the parameters and data formats of the product prior to full validation.

2 OBJECTIVES OF CAL/VAL

During the post-launch Cal/Val (Calibration/Validation) Phase of SMAP there are two objectives for each science product team:

- Calibrate, verify, and improve the performance of the science algorithms, and
- Validate accuracies of the science data products as specified in the Level 1 (L1) science requirements according to the Cal/Val timeline.

The process is illustrated in Figure 2.1. In this Assessment Report the progress of the L4_C team in addressing these objectives for beta release is described. The approaches and procedures utilized follow those described in the SMAP Cal/Val Plan [Jackson et al. 2012] and Algorithm Theoretical Basis Document for the Level 4 Carbon Data Product [Kimball et al. 2012].

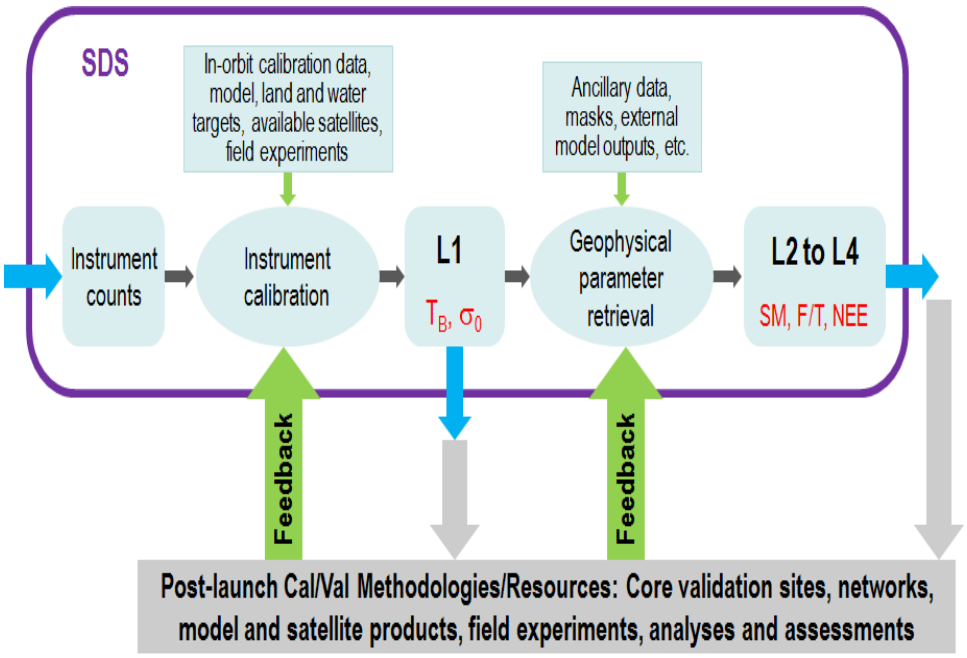

Figure 2.1. Overview of the SMAP Cal/Val Process.

SMAP established a unified definition base in order to effectively address the mission requirements. These are documented in the SMAP Handbook/ Science Terms and Definitions [Entekhabi et al. 2014], where Calibration and Validation are defined as follows:

- *Calibration*: The set of operations that establish, under specified conditions, the relationship between sets of values or quantities indicated by a measuring instrument or measuring system and the corresponding values realized by standards.
- *Validation:* The process of assessing by independent means the quality of the data products derived from the system outputs.

The L4_C product does not have a documented L1 accuracy requirement; instead the L4_C team adopted a self-imposed accuracy requirement threshold of 1.6 g C m^{-2} d^{-1} or 30 g C m^{-2} yr^{-1} (RMSE) for the bias-adjusted model NEE outputs, emphasizing northern (≥45°N) ecosystems, and at the level of observation uncertainty from tower eddy covariance monitoring sites (Baldocchi 2008).

In order to ensure the public's timely access to SMAP data, before releasing validated products the mission is required to release beta-quality products. The maturity of the products in the beta release is defined as follows:

- Early release is used to gain familiarity with data formats.
- The beta release is intended as a testbed to discover and correct errors.
- The beta release is minimally validated and still may contain significant errors.
- The general research community is encouraged to participate in the quality assessment and validation, but need to be aware that product validation and quality assessment (QA) are ongoing.
- Data may be used in publications as long as the fact that it is beta quality is indicated by the authors. Drawing quantitative scientific conclusions is discouraged. Users are urged to contact science team representatives prior to use of the data in publications, and to recommend members of the instrument teams as reviewers.
- The estimated uncertainties will be documented.

- The beta release data may be replaced in the archive when an upgraded (provisional or validated) product becomes available.

Due to the initially favorable quality of the SMAP observations and Level 4 model data assimilation system, this beta release of the L4_C product is closer to a provisional release, which is defined as:

- Incremental improvements are ongoing. Obvious artifacts or errors observed in the beta product have been identified and either minimized or documented.
- General research community is encouraged to participate in the QA and validation, but need to be aware that product validation and QA are ongoing.
- Product may be used in publications as long as provisional quality is indicated by the authors. Users are urged to contact science team representatives prior to use of the data in publications, and to recommend members of the instrument teams as reviewers.
- The estimated uncertainties will be documented.
- The provisional release data will be replaced in the archive when an upgraded (validated) product becomes available.

In assessing the maturity of the L4_C product, the L4_C team also considered the guidance provided by the Committee on Earth Observation Satellites (CEOS) Working Group on Calibration and Validation (WGCV):

- Stage 1: Product accuracy is assessed from a small (typically < 30) set of locations and time periods by comparison with *in situ* or other suitable reference data.
- Stage 2: Product accuracy is estimated over a significant set of locations and time periods by comparison with reference *in situ* or other suitable reference data. Spatial and temporal consistency of the product and with similar products has been evaluated over globally representative locations and time periods. Results are published in the peer-reviewed literature.
- Stage 3: Uncertainties in the product and its associated structure are well quantified from comparison with reference *in situ* or other suitable reference data. Uncertainties are characterized in a statistically robust way over multiple locations and time periods representing global conditions. Spatial and temporal consistency of the product and with similar products has been evaluated over globally representative locations and periods. Results are published in the peer-reviewed literature.
- Stage 4: Validation results for stage 3 are systematically updated when new product versions are released and as the time-series expands.

For the beta release the L4_C team's Stage 1 and Stage 2 (global assessment) activities have been established and are relatively mature. These Cal/Val program activities will continue toward validated release, including analyses of longer data records and updates from planned calibration refinements. These activities will continue through all Cal/Val stages over the SMAP mission life span.

3 EXPECTED L4_C ALGORITHM AND PRODUCT PERFORMANCE

The L4_C algorithm performance, including variance and uncertainty estimates of model outputs, was determined during the mission pre-launch phase through spatially explicit model sensitivity studies using available model inputs similar to those currently being used for operational production and evaluating the resulting model simulations over the observed range of northern (≥45 °N) and global conditions (Kimball et al. 2012, Entekhabi et al. 2014). The L4_C algorithm options were also evaluated during the mission prelaunch phase, including deriving canopy fPAR (fraction of photosynthetically active radiation absorbed by the canopy) from lower order NDVI (Normalized Difference Vegetation Index) inputs in lieu

of using MODIS (MOD15) fPAR; and including an explicit model representation of boreal fire disturbance recovery impacts. These results indicated that the L4_C accuracy requirements (i.e. NEE RMSE ≤ 30 g C m^{-2} yr^{-1}) could be met from the baseline algorithms over more than 82% and 89% of global and northern vegetated land areas, respectively (Yi et al. 2013, Kimball et al. 2012).

The global L4_C algorithm error budget for NEE derived during the mission prelaunch phase indicated that the estimated NEE RMSE uncertainty is proportional to GPP and is therefore larger in higher biomass productivity areas, including forests and croplands. Likewise, NEE RMSE uncertainty is expected to be lower in less productive areas, including grasslands and shrublands. Expected model NEE RMSE levels were also generally within targeted accuracy levels (NEE RMSE ≤30 g C m^{-2} yr^{-1}) for characteristically less productive boreal and Arctic biomes, even though relative model error as a proportion of total productivity (NEE RMSE / GPP) may be large in these areas. The estimated NEE uncertainty was lower than expected in some warmer tropical high biomass productivity areas (e.g. Amazon rainforest) because of reduced low temperature and moisture constraints to the L4_C respiration calculations so that the bulk of model uncertainty is contributed by GPP in these areas. Model NEE uncertainty in the African Congo was estimated to be relatively larger than in Amazonia due to relatively drier climate conditions in central Africa and associated larger uncertainty contributions of soil moisture and temperature inputs to the model respiration and GPP calculations.

4 L4_C PROCESSING OPTIONS

The current beta-release L4_C baseline product reflects various processing options that are implemented in the algorithm preprocessing stage for handling of the daily model inputs. These processing options are distinct from other options that are more internal to the model algorithms (Kimball et al. 2012). Two major preprocessing options are used in the L4_C beta-release product, namely, the use of estimated clear-sky fPAR inputs for missing or lower quality MODIS fPAR inputs, and the use of GMAO surface temperature fields to estimate frozen temperature constraints to the GPP calculations instead of SMAP FT defined constraints. The use of these preprocessing options are noted in the L4_C product bit flags as defined in the product specification document (Glassy et al. 2015).

The preprocessing options used in the beta-release product include a grid cell-wise selection of a MODIS fPAR 8-day climatology value where there data quality flag information from the operational MODIS fPAR inputs indicate missing or lower quality (QC) cloud contaminated data. The static MODIS global fPAR climatology is part of the ancillary data used for L4_C processing and was derived on a per grid-cell basis as the mean fPAR value for each 8-day time step over an annual cycle as determined from the best QC MODIS MOD15 fPAR long-term (2000-2012) record. The spatial extent of the global MODIS fPAR climatology also defines the global L4_C product domain. The use of the fPAR screening process and climatology generally improves model performance, especially in areas with persistent cloud cover, including the tropics and northern boreal/Arctic ecosystems. However, frequent substitution of current fPAR retrievals for alternative climatological values established from a long-term historical record may degrade model sensitivity to seasonal and annual climate variations, impacts for recent climate trends and extreme events, and recent land use and land cover changes. The fPAR quality bit flag information in the L4_C product provides a record of the spatial distribution and temporal frequency of these substitutions and facilitates future studies to evaluate these impacts.

The L4_C beta-product includes the use of a land surface temperature-defined FT frozen flag to define frozen temperature constraints to the model GPP calculations (Kimball et al. 2012). The FT frozen temperature flag is obtained from the lower order SMAP L3_SM_A inputs when available; when the L3_SM_A inputs are missing the FT frozen flag information is obtained from similar daily surface temperature inputs from the GMAO GEOS-5 land model, where temperatures below a 0.0°C threshold are defined as frozen. The major impact of using temperature-defined frozen flags from the land model is

that the FT flags are derived from relatively coarse simulations that are not directly informed by SMAP observations. Future L4_C product releases will benefit from FT frozen constraints defined from SMAP microwave retrievals with enhanced L-band sensitivity to landscape FT dynamics. These updates are expected to have the greatest benefit in northern ecosystems with greater frequency of frozen conditions, and in complex terrain and during seasonal FT transitions with larger FT spatial heterogeneity (Du et al. 2014). The use of SMAP FT inputs will also enhance SMAP carbon cycle science objectives encapsulated by the L4_C product, including improving understanding of the net carbon sink in boreal ecosystems (Entekhabi et al. 2010).

5 APPROACH FOR L4_C CAL/VAL: METHODOLOGIES

Validation is critical for accurate and credible product usage and must be based on quantitative estimates of uncertainty. For satellite-based retrievals, validation should include direct comparison with independent correlative measurements. The assessment of uncertainty must also be conducted and presented to the community in normally used metrics in order to facilitate acceptance and implementation.

During the mission definition and development period, the SMAP Science Team and Cal/Val Working Group identified the metrics and methodologies that would be used for L2-L4 product assessment. These metrics and methodologies were vetted in community Cal/Val Workshops and tested in SMAP pre-launch Cal/Val rehearsal campaigns. The methodological elements identified and their general roles are:

1. Core Validation Sites: Accurate estimates of products at matching scales for a limited set of conditions
2. Sparse Networks: One point in the grid cell for a wide range of conditions
3. Satellite Products: Estimates over a very wide range of conditions at matching scales
4. Model Products: Estimates over a very wide range of conditions at matching scales
5. Field Campaigns: Detailed estimates for a very limited set of conditions

In the case of the L4_C data product, all of the above elements can contribute to product assessment and improvement. With regard to the CEOS Cal/Val stages, Core Validation Sites address Stage 1 and Satellite and Model Products are used for Stage 2 and beyond. Sparse Networks fall between these two stages. The above methodological elements 1-4 were engaged in preparation for the L4_C beta-release. However, all of these elements will be further engaged in preparation for the validated product release.

6 PROCESS USED FOR BETA RELEASE

In order to meet requirements for a November 2015 L4 product beta-release, the SMAP L4_C team generally confined the product assessment to the April 13-July 30, 2015 product record. April 13, 2015 represents the beginning of the L4_C product series, while the designated end date was selected to allow sufficient time for analysis and preparation of the Beta Release Assessment Report. The team has been conducting frequent assessments of the L4_C operational product outputs and will continue to do this throughout the intensive Cal/Val phase and beyond.

Frequent product performance and validation assessments were conducted over the initial 3.5 month record using tower eddy covariance measurement-based daily CO_2 flux observations from up to 30 participating CVS tower sites. These comparisons involved spatially and temporally collocated daily tower observations and L4_C product outputs emphasizing NEE and GPP variables. Model performance was also evaluated against daily climatologies of the estimated carbon variables derived from long-term (2000-2013) MODIS fPAR and GEOS-5 (NRv4) surface meteorology records. The CVS comparisons

involved periodic teleconferences with the participating tower PIs to solicit local expertise in evaluating and interpreting product results in context with the tower observations and associated uncertainty.

Model and product performance was also evaluated using more extensive historical daily tower observations from 228 globally distributed sites represented by the FLUXNET La Thuille synthesis dataset (Baldocchi 2008). Model estimated NEE RMSE performance was evaluated against the range of observed NEE variability over the global domain and within the major plant functional type (PFT) classes represented by multi-year tower observational records spanning a large global range of vegetation and climate conditions.

The L4_C assessment activities included consistency checks against similar carbon variables available from other independent global data products, including the MODIS (Collection 5) MOD17A2 GPP record (Zhao and Running, 2010) and the MPI-MTE global GPP record (Jung et al. 2010). A global monthly composited SIF (solar-induced canopy fluorescence) observation record derived from the ESA GOME-2 sensor (Joiner et al. 2013) was also used as a GPP proxy for evaluating estimated global patterns and latitudinal gradients in the L4_C GPP calculations.

The L4_C product beta-release was determined on the basis of achieving a minimum set of satisfactory model and product performance metrics. These metrics involved: 1) demonstrations that the L4_C product outputs are consistent with known global and seasonal patterns, and that the magnitudes of estimated carbon fluxes are within realistic ranges for the major global PFT classes represented; 2) demonstrations that model performance is within design specifications, with no apparent model errors or anomalies.

7 ASSESSMENTS

7.1 Global Patterns and Features

General global patterns and seasonal dynamics of the major L4_C product fields were evaluated prior to more robust quantitative assessments of product performance and accuracy. These qualitative assessments were used to evaluate whether the product outputs capture characteristic global patterns and seasonality as well as impacts from known climate anomalies, including major droughts, occurring within the 2015 record. These qualitative assessments were also used to determine whether there were any apparent model errors or anomalies requiring more detailed model and product error diagnostics. The L4_C model processing is conducted at a daily time step and 1-km spatial resolution consistent with MODIS fPAR and land cover (PFT) inputs. The L4_C product outputs are posted to a 9-km resolution global EASE-grid (version 2) consistent with the SMAP Level 4 daily soil moisture (L4_SM) inputs. The primary daily product fields include vegetation gross primary production (GPP) and underlying environmental constraint (EC) metrics representing the proportional (%) reduction in estimated light-use efficiency (LUE) from potential conditions due to unfavorable environmental effects, including high vapor pressure deficits, cold daily minimum air temperatures, low soil moisture levels and frozen soil conditions (Kimball et al. 2012). The L4_C product fields also include heterotrophic respiration (Rh) and underlying soil moisture (Wmult) and soil temperature (Tmult) EC metrics. The primary carbon variable used for L4_C validation assessment is net ecosystem CO_2 exchange (NEE), which is computed as a residual difference between GPP and ecosystem respiration defined as the sum of Rh and estimated autotrophic respiration.

The L4_C GPP outputs are presented in **Figure 7.1** for two selected days in early and mid-spring of 2015. These results also show the corresponding EC constraints on estimated LUE and GPP for each day.

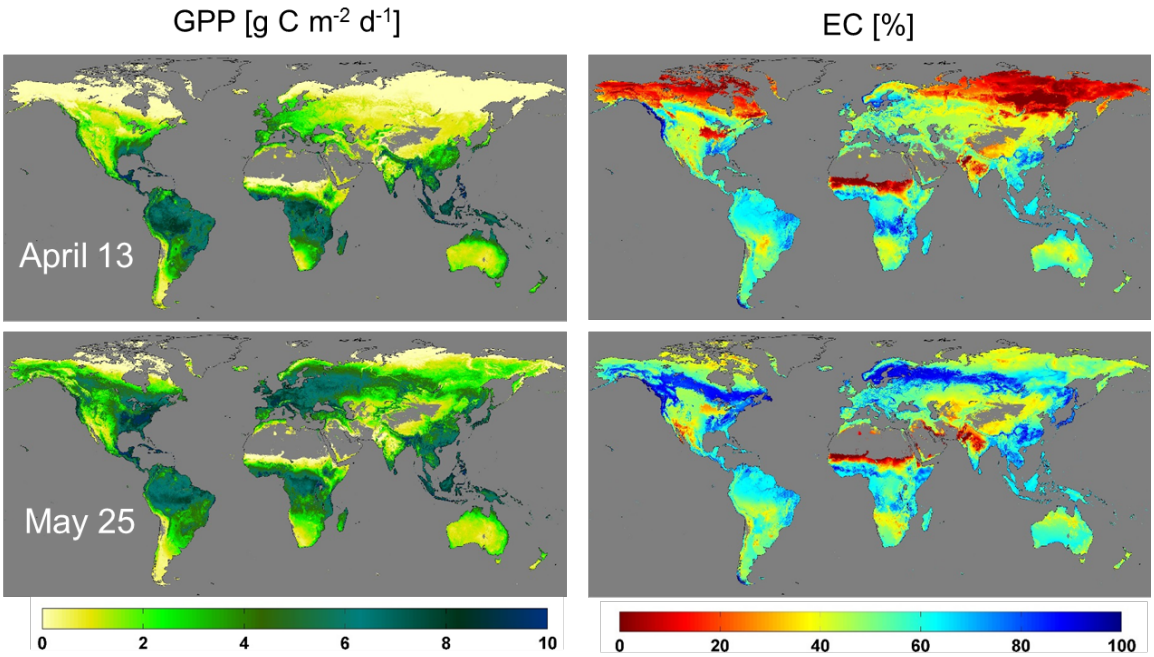

Figure 7.1. L4_C daily product examples for April 13th and May 25th, 2015, showing vegetation gross primary production (GPP) and the EC metric, which is the proportion (%) of estimated light use efficiency relative to a potential maximum rate (LUE/LUE_{mx}) defined for optimal (non-limiting) environmental conditions. Grey areas denote barren land, permanent ice, open water and other areas outside of the model domain.

These results depict the expected south-north progression of the Northern Hemisphere spring growing season onset and vegetation greening wave. Early spring conditions depicted by the April 13 map show low productivity (GPP) over the northern latitudes from widespread cold temperatures and associated strong EC restrictions. In contrast, much higher productivity levels occur over the northern latitudes in the May 25th image due to relatively warm, moist conditions and associated relaxation of EC constraints on LUE. Other regional anomalies are also apparent in these images, including relatively low GPP levels and large EC restrictions over northern India resulting from a documented 2015 spring heat wave. Lower productivity areas are also apparent over the southwest USA and African Sahel due to seasonal drought-induced soil moisture restrictions on estimated productivity. These results also show characteristic higher productivity over the tropics, indicating successful model screening and substitution of missing and cloud contaminated MODIS fPAR inputs using alternative clear-sky values from the ancillary MODIS 8-day fPAR climatology in the L4_C preprocessor.

Figure 7.2 depicts the L4_C model-estimated soil heterotrophic respiration (Rh) for the same two days in early to mid-spring 2015. The underlying cold temperature and low surface soil moisture EC constraints to the Rh calculation are also presented. These results show characteristically low respiration rates in early spring at higher latitudes prior to seasonal thawing, as indicated by strong Tmult reductions in the April 13th image. In contrast, the Tmult constraints are relaxed after seasonal thawing with the arrival of warmer temperatures, resulting in widespread increases in Rh rates indicated in the May 25th image. However, the potential increase in Rh is offset over many areas by surface soil moisture drying, including semi-arid areas of the southwest USA, southern Africa, and central Australia.

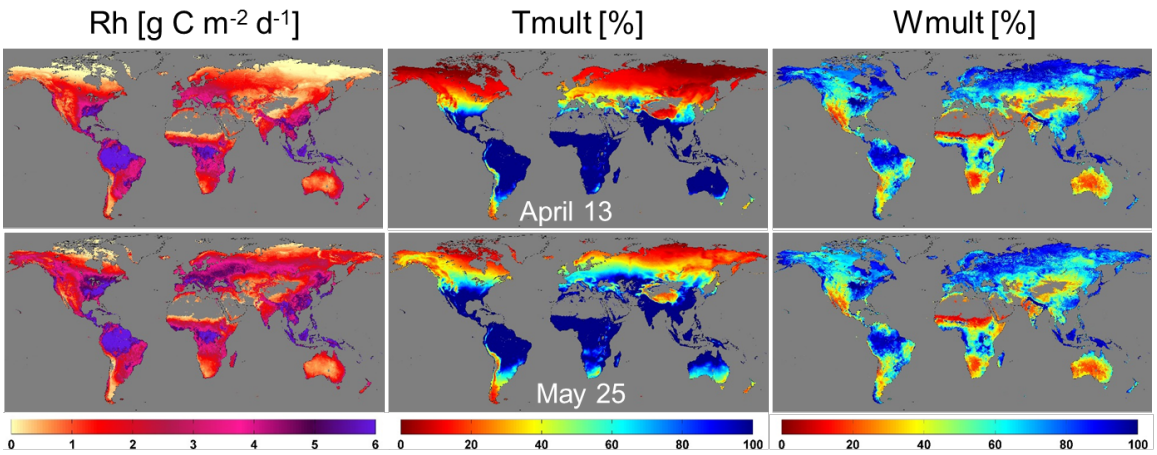

Figure 7.2. L4_C daily product examples for April 13th and May 25th, 2015, showing estimated soil heterotrophic respiration (Rh) and underlying surface soil temperature and soil moisture EC controls (Tmult, Wmult). The Tmult and Wmult EC metrics are dimensionless scalars ranging from 0 (fully constrained) to 100% (no constraint). Grey areas denote barren land, permanent ice, open water and other areas outside of the model domain.

A selection of L4_C estimated daily NEE images extending from mid spring to early summer is presented in **Figure 7.3**. These maps show relatively large characteristic spatial heterogeneity in the sign and magnitude of the estimated carbon fluxes because NEE is a residual difference between much larger GPP and respiration fluxes. GPP and ecosystem respiration also tend to respond similarly to environmental changes, which can obscure more obvious environmental impacts affecting carbon source/sink activity. Nevertheless, the sequence of images depicts the seasonal transition from early spring carbon source activity in the northern latitudes to widespread carbon sink activity with the arrival of warmer temperatures and vegetation greening in summer. Generally stronger carbon sink activity is also depicted over Eurasia relative to North America during the summer season due to anomalous warm, dry conditions reported over northwest Canada and Alaska in 2015. Likewise, the southwest USA and California show widespread and persistent carbon source activity stemming from an extended and severe drought in these areas.

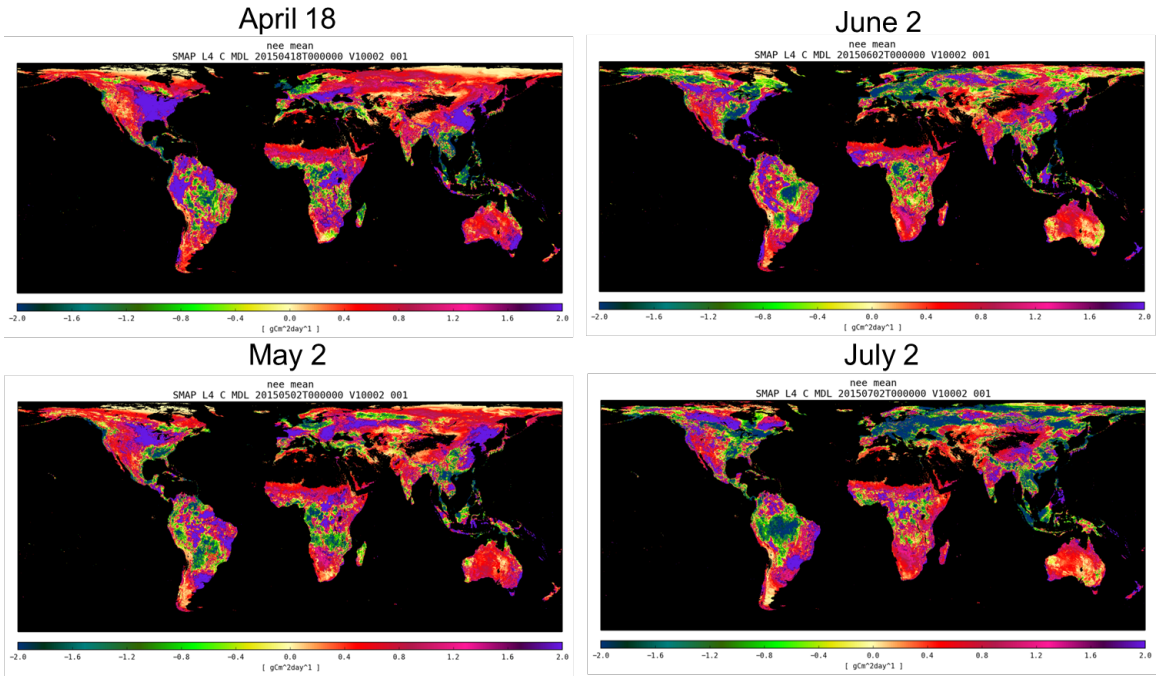

Figure 7.3. L4_C estimated NEE (g C m^{-2} d^{-1}) for four selected days between April 18th and July 2nd, 2015. Positive (negative) NEE fluxes denote net ecosystem carbon source (sink) activity. Black colors denote barren land, permanent ice, open water and other areas outside of the model domain.

The L4_C surface soil organic carbon (SOC) field from the initial (April 2015) portion of the operational record is presented in **Figure 7.4**. The L4_C algorithms use a general three-pool soil decomposition model with cascading litter quality and associated soil decomposition rates encompassing variable turnover rates for labile, cellulosic and recalcitrant organic matter pools (Kimball et al. 2012, Yi et al. 2013). The SOC map in the figure represents the aggregation of these three soil carbon pools. These initial results largely represent carbon model spin-up conditions that reflect the daily climatological (2000-2013) forcing conditions from the GMAO SMAP Nature Run version 4 (NRv4) system used to initialize the L4_C model, including its SOC state at the beginning of the SMAP operational record. The observed SOC patterns generally capture the expected characteristic soil carbon distributions, including higher SOC stocks in cold northern boreal forest and tundra biomes estimated to hold more than half of the global soil carbon reservoir (Hugelius et al. 2014). The L4_C SOC map also shows relatively high soil carbon storage in temperate forest areas due to high forest productivity rates and cool, moist soils that promote soil carbon storage. Low SOC areas occur over drier climate zones, including desert areas in the southwest USA with generally low productivity levels, warmer climate conditions and associated low SOC accumulations. The L4_C results also show relatively low SOC levels in tropical forests; high characteristic GPP rates and associated litterfall inputs are generally offset by warm, moist soil conditions that promote rapid decomposition in the soil, so that the majority of terrestrial carbon storage in the tropics is in vegetation biomass (Baccini et al. 2012).

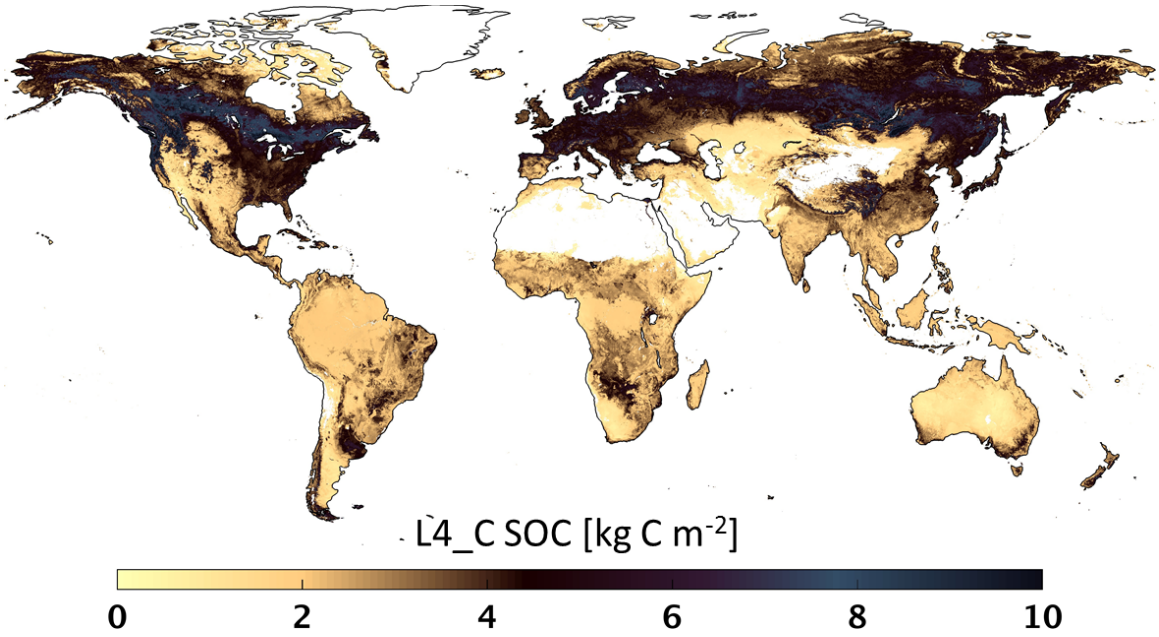

Figure 7.4. Estimated surface (< 10 cm depth) soil organic carbon (SOC, kg C m^{-2}) for April, 2015 from the SMAP L4_C operational record. The SOC estimates are derived at a 1-km spatial resolution during L4_C processing and posted to a 9-km resolution spatial grid. White areas denote barren land, permanent ice, open water and other areas outside of the model domain.

7.2 Global Performance against Historical Tower Observations

The L4_C validation assessment included comparisons of the model estimated daily carbon fluxes with ground-based observations of these variables from global sparse network tower eddy covariance CO_2 flux measurement sites as described in the SMAP Calibration/Validation Plan (Jackson et al. 2012). *In situ* data are critical in the assessment of the SMAP products. These comparisons provide for model performance and accuracy estimates and serve as a basis for modifying algorithms and/or parameters. A robust analysis requires many sites representing a diverse range of vegetation and climate conditions. The L4_C assessment included comparisons of L4_C estimates of daily NEE and GPP against spatially collocated, gap-filled daily observations of these parameters from 228 tower sites spanning the global domain and representing the major global PFT classes. The tower records were obtained from a larger set of tower site records from the FLUXNET La Thuile tower data synthesis (Baldocchi 2008). The tower sites enlisted for the comparisons were selected on the basis of being located within relatively homogenous terrain and land cover (PFT) areas defined from MODIS 1-km land cover data within 9km x 9km windows centered over each tower site. The tower sites were also selected on the basis of having multi-year observational records with relatively well characterized observation uncertainty.

The La Thuile tower record represents a global synthesis of FLUXNET daily tower observations where tower measurement records have been processed using consistent methods for temporal gap-filling of missing data, aggregation of daily carbon fluxes, and partitioning of NEE into component carbon fluxes. However, the La Thuile data record only extended to 2007, so that comparisons with the L4_C product outputs were spatially co-located but were not temporally consistent. Therefore, these comparisons focused on evaluating L4_C-based NEE and GPP performance in relation to historical daily means and temporal variability (SD) at the 228 globally representative tower sites.

We conducted a spatial implementation of the L4_C error budget to map estimated ubRMSE performance for the NEE estimates over the global domain. Spatially explicit estimates of NEE ubRMSE

(g C m^{-2} yr^{-1}) were derived using a locally weighted forward model sensitivity analysis (Kimball et al. 2014) driven by MODIS fPAR and GMAO SMAP NRv4 daily surface meteorology inputs. The NRv4 data is derived using the same GEOS-5 land model underpinning the SMAP Level 4 Soil Moisture (L4_SM) product; these data were also used for calibration and initialization of the L4_C operational algorithms. The resulting global NEE error budget is presented in **Figure 7.5**. The figure depicts the tower sites used for the model performance assessment and includes a summary plot showing the mean and range of variability in the correlations between the global tower NEE observations and associated L4_C NEE estimates stratified according to PFT class. The number of tower sites (N) represented within each PFT class is shown at the top of the plot, while NEE ubRMSE estimates are summarized for all land areas within each PFT class and in relation to the observed RMSE and ubRMSE differences and NEE correlations with the tower observations representing each PFT class. These results indicate that approximately 66% and 83% of the global and northern (≥45°) domains are within the targeted L4_C product performance threshold for NEE (ubRMSE≤30 g C m^{-2} yr^{-1}). The estimated ubRMSE global performance is largely consistent with local assessments derived from tower NEE observations representing the major PFT classes. The magnitude of the NEE RMSE differences are proportional to ecosystem productivity (GPP) so that more productive sites such as croplands have generally greater RMSE levels than less productive (e.g. shrubland and grassland) areas. Thus, if we express the NEE RMSE as a proportion of the NEE flux, the estimated extent of meaningful NEE estimates (i.e., $|ubRMSE/NEE| < 30\%$) increases to more than 80% of the global domain. Correlations between the model and tower NEE observations are generally greater in areas with larger characteristic seasonality, while EBF areas have lower correspondence largely due a smaller seasonal cycle in these predominantly tropical areas. Over northern land areas NEE ubRMSE levels are generally within the targeted accuracy threshold, except for some northern croplands and forests. Overall, these results indicate that the L4_C algorithms and beta-product are consistent with expected model design and performance specifications.

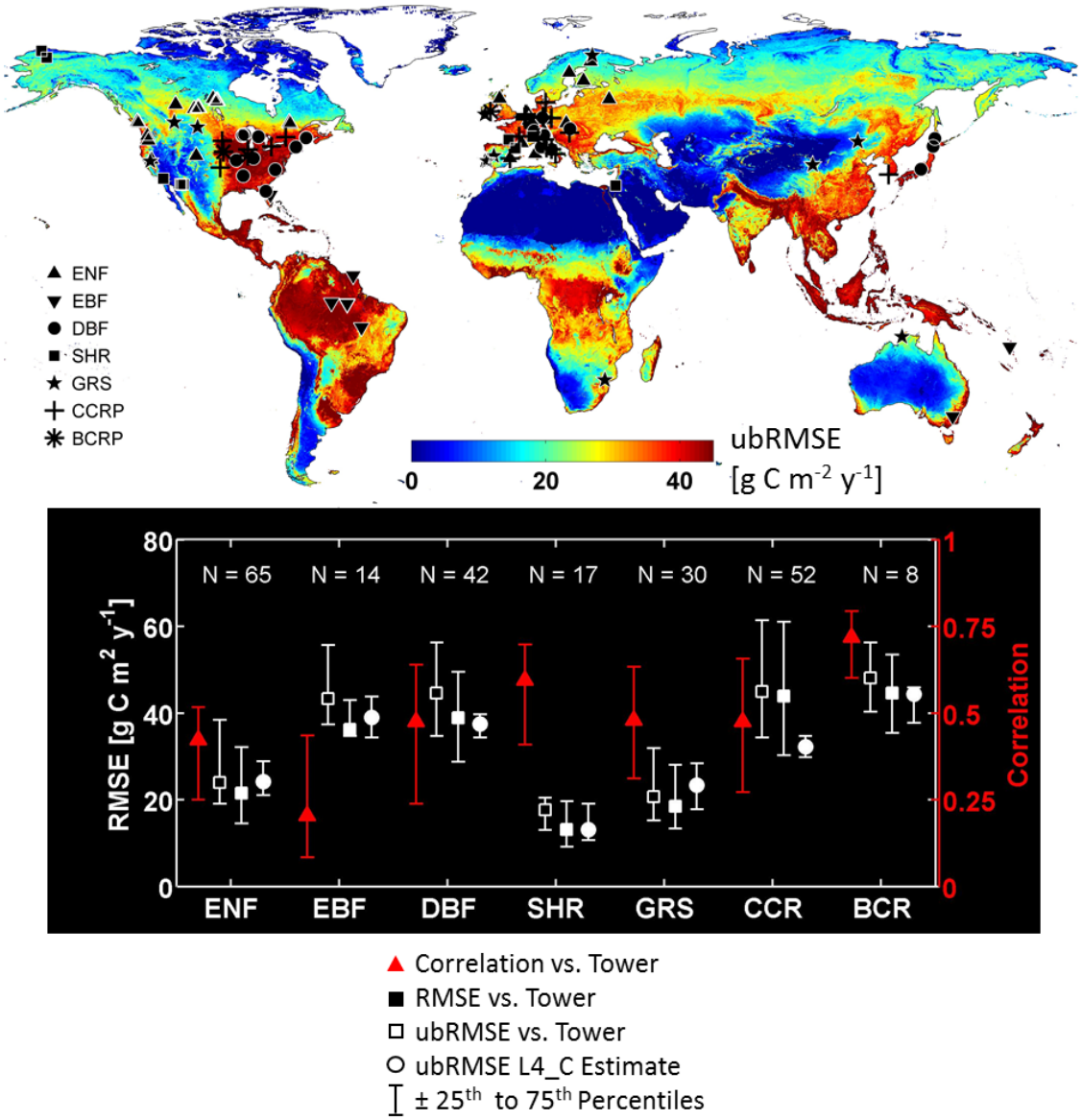

Figure 7.5. Estimated L4_C model and product performance for NEE in relation to in situ observations from 228 tower sites representing the major global plant functional type (PFT) classes, including evergreen needleleaf forest (ENF), evergreen broadleaf forest (EBF), deciduous broadleaf forest (DBF), shrubland (SHR), grassland (GRS), cereal (C3) croplands (CCR) and broadleaf (C4) croplands (BCR). The tower sites are depicted in the L4_C model-estimated NEE ubRMSE (g C m^{-2} yr^{-1}) map (top). The lower plot includes a summary of mean model and tower NEE correlations and RMSE differences within each PFT class, with associated 25th and 75th percentiles of spatial variability; the number (N) of tower observation sites represented within each PFT class is denoted at the top of the plot. The estimated mean ubRMSE levels derived from the model sensitivity simulations (shown in upper map) for the tower pixel locations are also summarized within each PFT class in the plot.

We also compared L4_C outputs from the initial operational record against daily mean GPP and NEE values from the historical tower observations; here L4_C outputs for the beta evaluation period (Apr 13 – Jul 30, 2015) were compared against similar daily mean carbon fluxes from the 228 historical tower site records for the same (Apr 13 – Jul 30) seasonal period. The resulting spatial mean and variability (SD) in daily RMSE differences of the tower site comparisons within each PFT class are presented in

Figure 7.6. Both total and unbiased RMSE values are presented. These results are similar to the global annual performance summary described above (**Figure 7.5**), except that the performance assessment is conducted only for a limited (Apr to Jul) seasonal period using MODIS fPAR and SMAP-informed operational environmental inputs to the L4_C algorithms. These results indicate that the L4_C performance for the initial beta evaluation period is consistent with the algorithm design and targeted daily NEE accuracy threshold (ubRMSE≤1.6 g C m^{-2} d^{-1}) for relatively less productive PFT classes characteristic of northern biomes, whereas croplands and deciduous broadleaf forests show higher RMSE levels consistent with characteristic higher productivity levels and NEE rates for these vegetation types. Surprisingly, the L4_C model and tower RMSE values are low for relatively productive tropical forests (EBF); however, the relatively few (14) towers representing this PFT class may not adequately represent global EBF diversity. The total RMSE levels are higher than the ubRMSE values due to systematic spatial and temporal bias in both model outputs and tower observations. The contributing sources and characteristics of model and tower bias are not well defined given the relatively short (Apr-Jul, 2015) operational record examined. Characterization of systematic bias is expected to improve with a longer operational record. The L4_C performance is also expected to improve with a longer SMAP observation record and associated calibration refinements, and reprocessing updates to the lower order sensor retrievals and L4 product outputs.

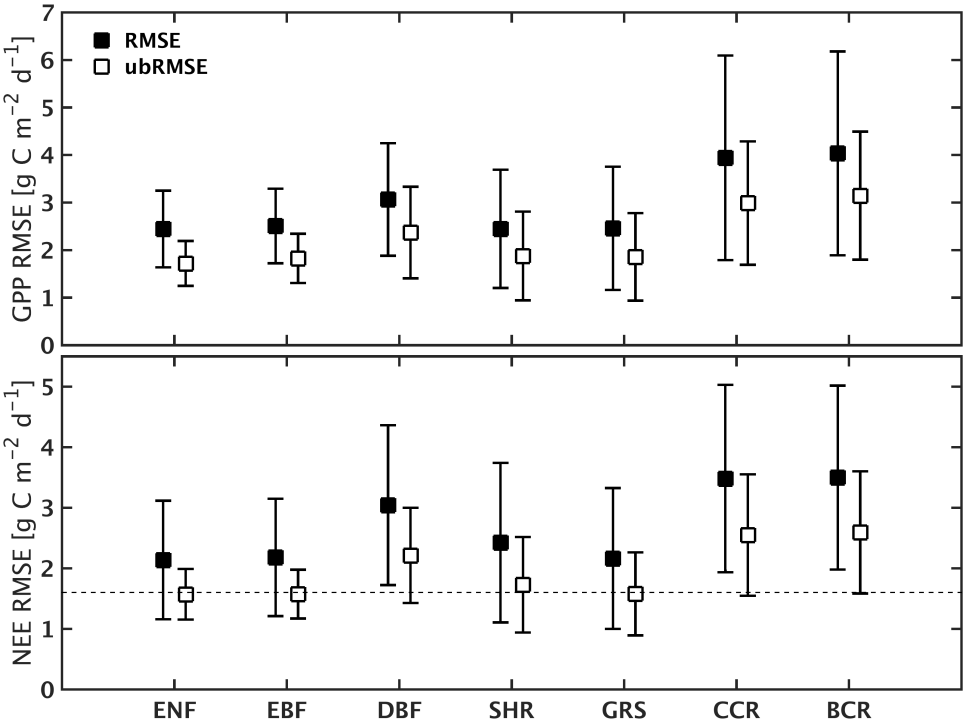

Figure 7.6. Spatial mean and variability (SD) in daily RMSE differences between L4_C operational outputs for GPP and NEE and daily mean C fluxes derived from historical daily tower observations at the 228 FLUXNET sites for the L4_C beta evaluation period (April 13 to July 30). The comparison results are summarized within global PFT classes representing individual tower sites. Both total (black squares) and bias-adjusted (white squares) RMSE values are presented. The targeted accuracy threshold for NEE (1.6 g C m^{-2} d^{-1}) is also shown (dashed line).

7.3 Core Validation Sites

The initial L4_C operational daily outputs (Apr 13 – Jul 30, 2015) were compared against in situ daily tower observations for up to 33 participating core tower validation sites. Unlike the historical site

comparisons described above, the CVS comparisons were both spatially consistent and temporally overlapping for the available 2015 record. The CVS comparisons are enabled by active participation from individual tower site principle investigators (PIs) in the SMAP L4_C Cal/Val process. The SMAP L4_C CVS sparse tower network is summarized in **Table 7.1**; the associated tower CVS locations are presented in **Figure 7.7** along with the FLUXNET sites used for L4_C calibration and performance assessments (**Section 7.2**).

Table 7.1. CVS sparse tower network used for intensive L4_C product assessments.

[1]Site	[2]PFT	Lat	Lon	Location	Full Name
FI-Sod	ENF	67.36	26.64	Finland	FMI Sodankyla
CA-Ojp	ENF	53.92	-104.69	Sask. CN	BERMS Old Jack Pine
CA-Obs	ENF	53.99	-105.12	Sask. CN	BERMS Southern Old Black Spruce
US-ICt	SHR	68.61	-149.30	AK, USA	Imnavait Tussock
US-ICh	SHR	68.61	-149.30	AK, USA	Imnavait Heath
US-ICs	SHR	68.61	-149.31	AK, USA	Imnavait Wet Sedge
US-BCr	ENF	64.70	-148.32	AK, USA	Bonanza Creek Black Spruce
US-BCb	ENF	64.70	-148.32	AK, USA	Bonanza Creek Bog
US-BCf	ENF	64.70	-148.31	AK, USA	Bonanza Creek Fen
US-PFa	DBF	45.95	-90.27	WI, USA	Park Falls
US-FPe	GRS	48.31	-105.10	MT, USA	Fort Peck
US-Atq	GRS	70.47	-157.41	AK, USA	Atqasuk
US-Ivo	SHR	68.49	-155.75	AK, USA	Ivotuk
US-Me2	ENF	44.45	-121.56	OR, USA	Metolius Intermediate Pine
US-Me3	SHR	44.32	-121.61	OR, USA	Metolius Second Young Pine
US-SO2	SHR	33.37	-116.62	CA, USA	Sky Oaks Old Stand
US-SO3	SHR	33.38	-116.62	CA, USA	Sky Oaks Young Stand
US-SO4	SHR	33.38	-116.64	CA, USA	Sky Oaks
US-SRM	SHR	31.82	-110.87	AZ, USA	Santa Rita Mesquite
US-Wkg	GRS	31.74	-109.94	AZ, USA	Walnut Gulch Kendall Grasslands
US-Whs	SHR	31.74	-110.05	AZ, USA	Walnut Gulch Lucky Hills Shrubland
US-Ton	SHR	38.43	-120.97	CA, USA	Tonzi Ranch
US-Var	SHR	38.41	-120.95	CA, USA	Vaira Ranch
AU-Whr	SHR	-36.67	145.03	Australia	Whroo
AU-Rig	CRP	-36.66	145.58	Australia	Riggs Creek
AU-Yan	CRP	-34.99	146.29	Australia	Yanco
AU-Stp	GRS	-17.15	133.35	Australia	Sturt Plains
AU-Dry	GRS	-15.26	132.37	Australia	Dry River
AU-DaS	GRS	-14.16	131.39	Australia	Daily River Savannah
AU-How	GRS	-12.50	131.15	Australia	Howard Springs
AU-GWW	SHR	-30.19	120.65	Australia	Great Western Woodlands
AU-ASM	SHR	-22.28	133.25	Australia	Alice Springs

AU-TTE	SHR	-22.29	133.64	Australia	Ti Tree East

[1]FLUXNET based tower site identifiers; [2]Tower PFT classes defined from a 1-km resolution MODIS (MOD12Q1) Type 5 global land cover map, consistent with L4_C processing.

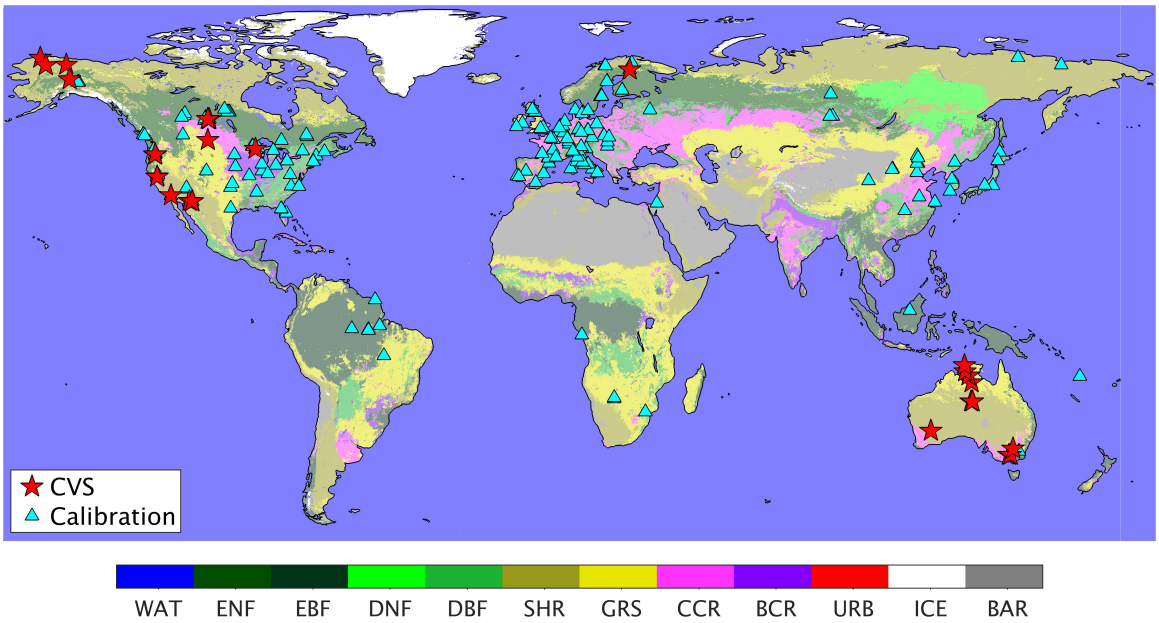

Figure 7.7. Locations of the core (CVS) tower validation sites used for intensive L4_C product assessments; FLUXNET sites with historical tower records used for the L4_C model calibration and performance assessments are also shown in relation to global plant functional types summarized from the MODIS MOD12Q1 (Type 5) global land cover classification.

Most of the CVS partners are providing near real-time daily tower observations, enabling temporally overlapping comparisons between the in situ tower observations and collocated SMAP L4_C operational product outputs. The CVS network spans 29 site locations and a broad range of climate and vegetation conditions; two of the sites (Imnavait, Bonanza Creek) include multiple towers sampling different vegetation communities within the larger sub-regions for a total of 33 participating CVS towers. Unlike the FLUXNET sites used for the L4_C global performance assessment (**Section 7.2**), the CVS towers may be located in spatially heterogeneous land cover areas with different PFT characteristics than the dominant vegetation class represented within the overlying 9-km resolution L4_C grid cell. Therefore, in addition to comparisons between tower observations and average daily model outputs for the corresponding overlying 9-km grid cell, the model-tower CVS assessment included comparisons between tower observations and (pre-aggregated, higher resolution) model output for the PFT within the cell that most closely represents the reported PFT within the local tower footprint. This is enabled by the 1-km resolution of the L4_C processing commensurate with the MODIS fPAR and PFT inputs; the sub-grid PFT outputs within each 9-km grid cell are preserved in the operational product outputs.

The initial CVS comparisons associated with the L4_C beta-release were limited to the Apr 15 – Jul 30, 2015, time period. The global distribution of CVS towers in both Northern and Southern Hemisphere locations allows for a relatively robust assessment of seasonality in the initial (Apr-Jul) record; environmental conditions were largely dormant at the northern high latitude tower sites in the post-launch early spring period, whereas the Southern Hemisphere tower sites were experiencing austral late summer and early fall conditions. Due to the CVS requirements for frequent (weekly) tower data delivery updates,

uncertainty in the CVS tower records is expected to be larger than would otherwise be expected from longer and more refined science data quality records. Local assessments of tower data quality were provided by many of the tower PIs as part of their data deliveries; the criteria and structure of the data quality metrics provided varied across the different tower sites, but they all give at least some qualitative indication of the reliability of the tower observations.

The L4_C performance assessment against CVS daily tower observations for NEE and GPP is presented in **Figure 7.8**. These results represent CVS sites having available tower observations within the beta evaluation period and are a subset of the full CVS network listed in **Table 7.1**. The reported metrics for each site include RMSE and mean residual bias computed between the tower observations and collocated model outputs representing daily mean carbon fluxes within the overlying 9-km resolution model grid cell; RMSE, bias and R^2 correspondence metrics are also derived for the model sub-grid PFT mean that is most similar to the reported local tower footprint PFT. The estimated bias-adjusted RMSE metrics are also presented. The initial CVS comparisons show several apparent tower site outliers, including Metolius, Bonanza Creek and Howard Springs. However, these outliers were largely traced to incorrect processing of the tower observations rather than to model error. Other outliers were caused by PFT mismatches between the local (~1-km^2) tower footprint observations and overlying L4_C model grid cells. For example, the Howard Springs tower footprint is characterized as woody savanna with a grass/shrub understory and Eucalyptus forest overstory. The MODIS MOD12Q1 Type 5 global land cover classification used for L4_C processing doesn't include a woody savanna PFT category; instead, the 9-km grid cell overlying the Howard Springs site is predominantly characterized as GRS, with smaller proportional DBF representation; neither of these PFT categories provides a close functional match with the local Howard Springs vegetation, leading to larger model-tower differences. Despite the anomalous outlier sites described above, the model-tower comparison results show generally favorable performance, with L4_C derived NEE outputs near the targeted RMSE level, including both total and bias-adjusted error metrics.

The initial CVS comparisons reveal several challenges associated with maintaining robust quality control over a diverse set of tower observations and participating Cal/Val partner teams, despite efforts to standardize data formatting and submission of frequent tower observation updates. The CVS tower observations have larger uncertainty relative to longer historical data records such as the La Thuile FLUXNET record (Section 7.2). The larger tower observation uncertainty is due to multiple factors, including project requirements for frequent updating of tower data, which restricts the amount of time available for detailed post-processing analysis and data quality checks. The relatively short (~3.5 mos) period of record of the initial CVS observations also contributes to larger uncertainty associated with gap-filling of missing data and estimation of component carbon fluxes (e.g. GPP) from the tower NEE measurements. While many of the tower partners have contributed tower data quality metrics, these data have not yet been incorporated into the CVS analysis. The CVS comparisons will continue to be updated and refined using longer data records acquired during the post-beta release period. The relative quality and reliability of the CVS comparisons is expected to improve with longer data records incorporating a full annual cycle and with further refinements to the L4_C Cal/Val matchup tools.

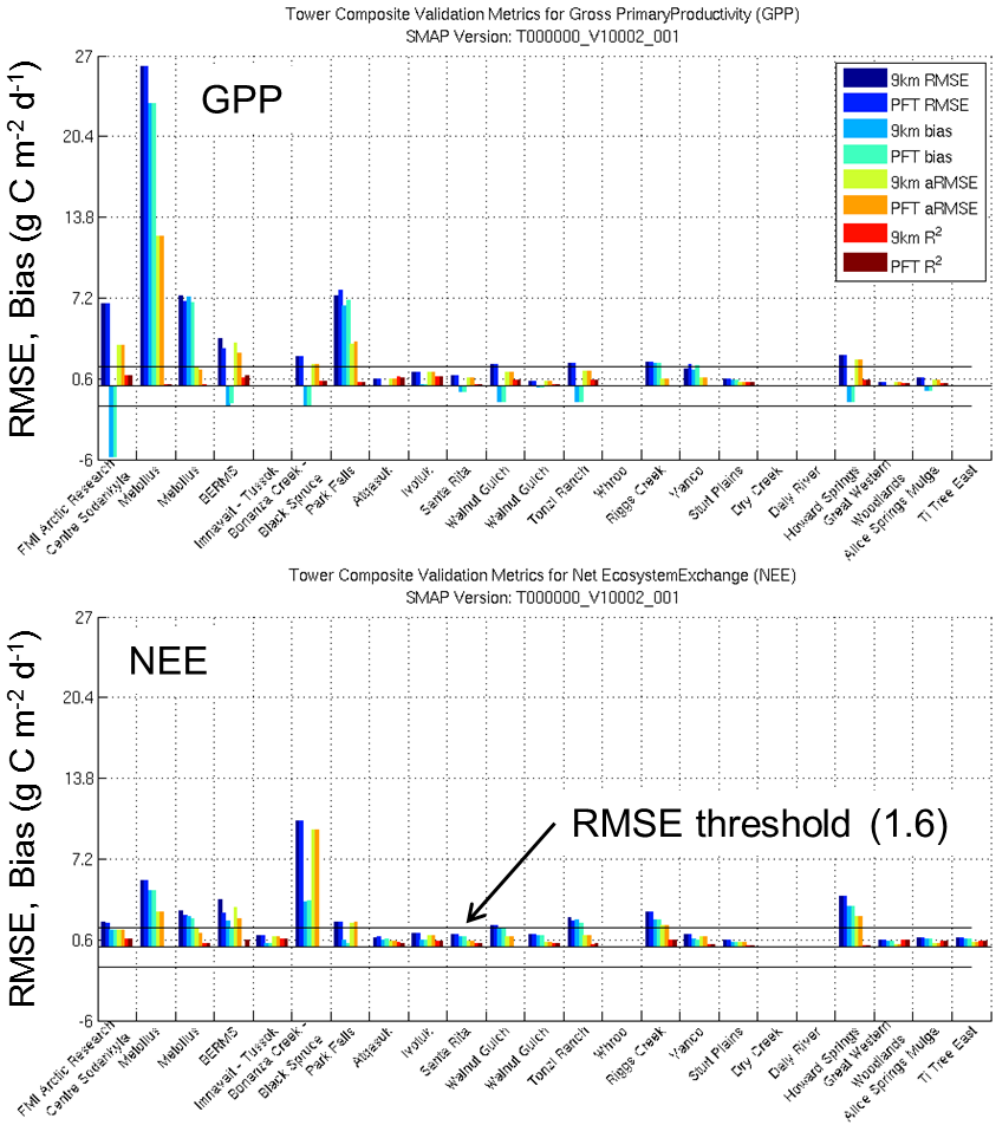

Figure 7.8. Summary of initial CVS comparisons between daily tower observations and L4_C daily product outputs for GPP and NEE from the April 15 – July 30, 2015 operational record. The reported metrics include R^2 correspondence, RMSE and bias between tower observations and L4_C spatial mean daily conditions within the overlying 9-km resolution product grid cell (9km R^2, 9km RMSE, 9km bias); RMSE, bias and R^2 correspondence between the tower observations and the most similar PFT mean within the 9-km grid cell (PFT RMSE, PFT bias, PFT R^2); and the associated bias-adjusted RMSE values (aRMSE). The targeted daily NEE RMSE threshold for the L4_C product (1.6 g C m^{-2} d^{-1}) is also shown.

7.4 Consistency with Other Global Carbon Products

The L4_C product outputs were compared against similar variables from other available global carbon products. The objective of these comparisons was to assess and document the general consistency of selected L4_C operational product fields in relation to similar variables from other global benchmark datasets commonly used by the community. The global data products examined are publicly available and include:

1) The NASA EOS MODIS MOD17A2 (C5) operational GPP product, with 1-km resolution and 8-day temporal fidelity (Zhao and Running, 2010);
2) The Max Planck Institute's Model Tree Ensemble (MPI-MTE)-based global tower observation upscaling of monthly GPP from the La Thuile FLUXNET synthesis observational record (Jung et al. 2010);
3) Solar-Induced canopy Fluorescence (SIF) observations from the ESA GOME-2 (Global Ozone Mapping Experiment) satellite sensor (Joiner et al. 2013);
4) Global soil organic carbon (SOC) inventory records from the International Geosphere Biosphere Program Data Information System (IGBP-DIS; Global Soil Data Task Group 2000) and the Northern Circumpolar Soil Carbon Database (NCSDC; Hugelius et al. 2014).

Global consistency checks between the selected L4_C outputs and these datasets involved comparing mean latitudinal distributions of average product fields for the April - July, 2015, period against average conditions for the similar period derived from the other historical data records. The MODIS MOD17A2 and MPI-MTE GPP records used for this analysis extended from 2000 to 2014 and from 2000 to 2011, respectively. The GOME-2 SIF record used for this study represented composited mean monthly observations extending from 2007-2013. Differences were computed between the L4_C GPP maps and the MOD17 and MPI-MTE GPP maps to evaluate the global distribution of differences in estimated productivity. The SIF retrieval from GOME-2 is related to LUE and photosynthesis and was used as an observational proxy for GPP.

The available SOC inventory records represent static maps extending over global (IGBP-DIS) and northern (NCSCD) domains. Surface (<10cm depth) SOC stocks were estimated as a fixed proportion (33.33%) of the total soil profile (0-100 cm depth) SOC stock records. These data were compared against the initial L4_C SOC product outputs from April, 2015. The SOC records were evaluated by comparing latitudinal means and spatial SD ranges. A global SOC difference map was also computed between the L4_C and IGBP-DIS records to evaluate the spatial pattern of SOC differences. Detailed summaries of these comparisons are provided in the following sub-sections.

7.4.1 MODIS MOD17 GPP

The L4_C daily GPP product fields were averaged over the April to July, 2015, period and compared against the MOD17A2 GPP climatological means for the same months, but derived from the long-term (2000-2014) MODIS record. The averaged MODIS GPP data was re-projected from a 5-km resolution geographic projection to the 9-km resolution global EASE-grid (V.2) format of the L4_C product using nearest-neighbor resampling. A GPP difference map was then computed by grid cell-wise subtraction of MOD17 values from collocated L4_C values. The distributions of the GPP spatial means and ±1 SD spatial variations were also computed along 0.05 degree latitudinal bins and compared for relative consistency between the MOD17 and L4_C datasets. These results are presented in **Figure 7.9**.

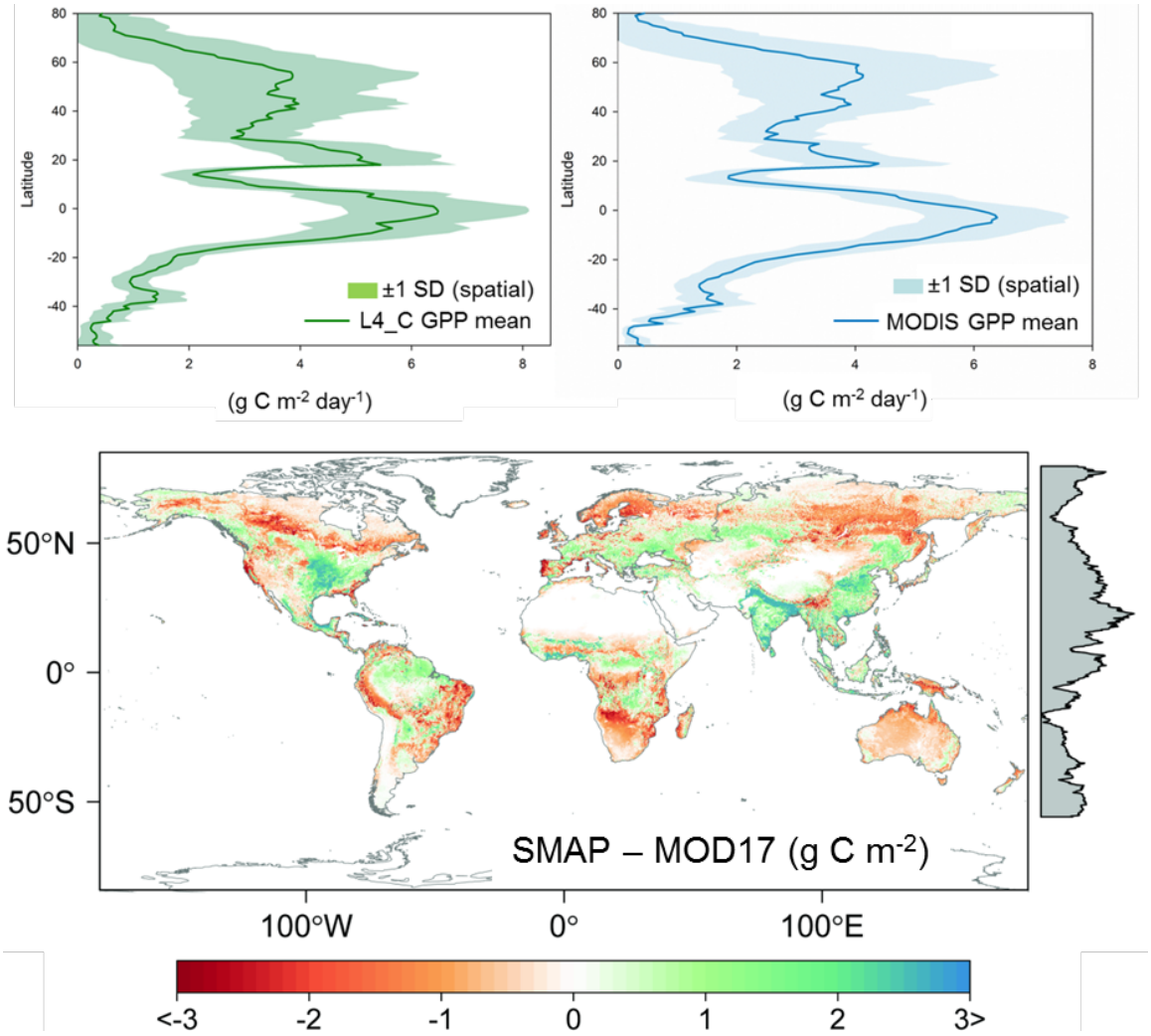

Figure 7.9. Comparison of mean daily GPP outputs (April to July; g C m^{-2} d^{-1}) from the SMAP L4_C and MODIS MOD17A2 (C5) global data products. The L4_C outputs are derived from the data record for 2015, while the MOD17A2 results represent climatological means derived from the long-term (2000-2014) MODIS record. The distributions of GPP spatial means and ±1 SD spatial variations are summarized within 0.05 degree latitudinal bins (top); the GPP difference map between the SMAP and MOD17 results is also shown (bottom) along with the relative mean latitudinal distribution of the GPP difference (grey shading along Y-2 axis). White areas in the difference map represent barren land, permanent ice, open water bodies and other areas outside of the L4_C product domain.

The L4_C GPP product fields for the initial (April – July, 2015) operational record examined show a global productivity distribution similar to that in the MODIS MOD17A2 GPP record. The resulting productivity patterns show generally similar magnitudes, latitudinal distributions and spatial variability. However, there are also significant regional differences that can be attributed to one or more factors, including differences in model calibrations and underlying environmental controls on estimated GPP, and differences between 2015 climate (the year used for the L4_C record) and that for 2000-2014 (used for the long-term MODIS climatology). Areas with relatively lower L4_C GPP levels (red colors) include northern boreal forests, the southwest USA, central Australia and the sub-tropics. These areas have generally significant seasonal dry periods where plant-available soil moisture limitations reduce productivity from potential conditions. The lower L4_C GPP levels in these areas reflect the impact of

including additional soil moisture constraints to productivity in the L4_C algorithms relative to the use of atmospheric VPD as the sole moisture constraint to productivity in the MOD17 LUE algorithm. Other areas with relatively lower L4_C productivity levels reflect documented dry climate anomalies in the 2015 record relative to the longer term climate conditions represented by the MOD17 record. These climate anomalies include ongoing drought conditions over California and the southwest USA and relatively warm, dry spring and summer 2015 conditions over boreal Alaska, the north central USA and Canada.

The GPP difference maps also show many areas with higher L4_C productivity levels (green colors) relative to the MOD17 GPP results. The L4_C results show generally higher productivity levels over the temperate zone, particularly over intensive cropland areas, including eastern China, India, and the central USA. These differences are largely attributed to improved calibration of C3 and C4 croplands in the L4_C LUE model relative to the MOD17 LUE model (Turner et al. 2006, Madani et al. 2014). The improved L4_C calibration in these areas partially reflects the use of a greater number of cropland tower sites in the model BPLUT calibration and the enhanced MODIS fPAR quality screening used during L4_C processing (Kimball et al. 2012). Other areas with relatively higher L4_C productivity rates reflect the influence of regional climate variations favoring greater productivity levels in 2015 relative to long-term average conditions represented by the MOD17 record; these areas include relatively higher productivity in response to an early thaw season over northern Alaskan tundra.

7.4.2 MPI-MTE GPP

The L4_C mean daily GPP product fields from the April to July, 2015, period were compared against the MPI-MTE GPP record averaged over the same months, but derived from the longer MPI-MTE monthly record extending from 2000-2011 (Jung et al. 2010). The MPI record is derived using a Model Tree Ensemble (MTE)-based machine learning algorithm and empirical upscaling of tower-based daily GPP observations from the global FLUXNET data archive. The MTE spatial upscaling approach also uses 29 explanatory geospatial variables, including monthly fPAR from the SeaWiFS sensor. The monthly MPI GPP data was re-projected from a 0.5 degree spatial resolution and geographic projection to the 9-km resolution global EASE-grid (V.2) format of the L4_C product using nearest-neighbor resampling. A GPP difference map was then computed by grid cell-wise subtraction of MPI values from collocated L4_C values. The distributions of the GPP spatial means and ±1 SD spatial variations were also computed along 0.05 degree latitudinal bins and compared for relative consistency between the MPI and L4_C datasets. These results are presented in **Figure 7.10**.

Consistent with the MOD17 comparison described above, the L4_C and MTE results show generally similar GPP magnitudes and latitudinal mean distributions, with generally higher producivity levels in the tropics and temperate zones and lower productivity levels at higher latitudes. However, the MTE results show lower GPP spatial heterogeneity as indicated by relatively narrow SD in the latitudinal distribution plots, especially over the lower latitudes and Southern Hemisphere. The narrower MTE range of variability is attributed to the limited number of global in situ tower sites used in the MTE spatial extrapolations; the global distribution of tower network sites is particularly sparse over the tropics and Southern Hemisphere land areas (Schimel et al. 2015).

As with the previous MOD17 comparison, the L4_C results indicate generally lower productivity than the MTE results over drier climate areas, including boreal forest and subtropical zones. These differences are attributed to the impact of dynamic soil moisture-related water supply constraints used in the L4_C GPP calculations; the MTE results are based on generalized precipitation and potential evapotranspiration indices used to define moisture-related impacts on productivity spatial patterns. The L4_C results also show generally lower GPP levels over the temperate zone, including tropical forest and cropland areas. The L4_C GPP levels in these areas are generally intermediate between MOD17 and MTE.

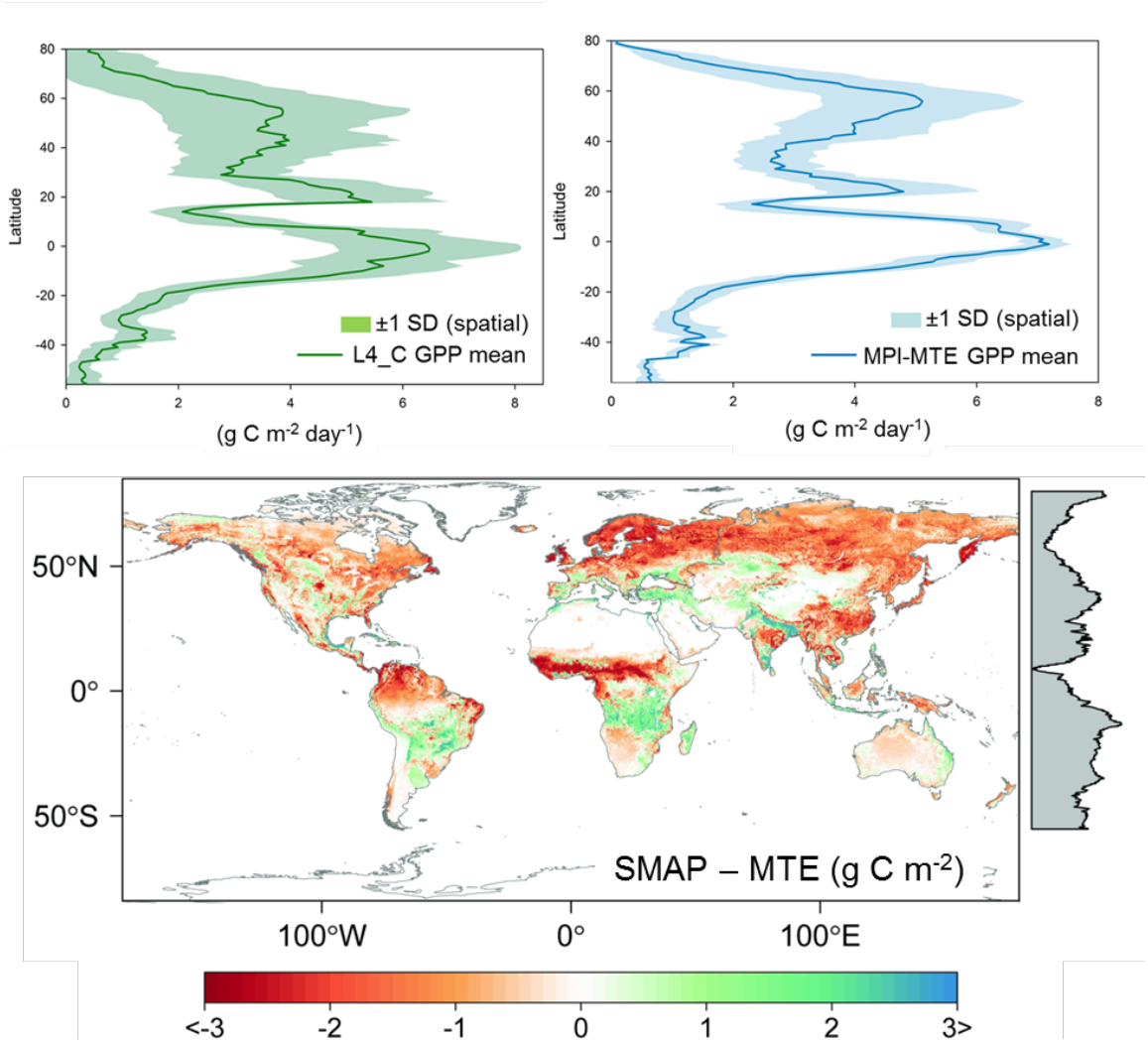

Figure 7.10. Comparison of mean daily GPP outputs (April to July; g C m^{-2} d^{-1}) from the SMAP L4_C and MPI-MTE global data products. The L4_C outputs are derived from the initial data record for 2015, while the MTE results represent climatological means derived from a long-term (2000-2011) monthly record. The distributions of GPP spatial means and ±1 SD spatial variations are summarized within 0.05 degree latitudinal bins (top); the GPP difference map between the SMAP and MTE results is also shown (bottom) along with the relative mean latitudinal distribution of the GPP differences (grey shading along Y-2 axis). White areas in the difference map represent barren land, permanent ice, open water bodies and other areas outside of the L4_C product domain.

7.4.3 GOME-2 SIF

The L4_C mean daily GPP product fields from the April to July, 2015, period were compared against satellite-based SIF observations averaged over the same months, but derived from the longer (2007-2013) GOME-2 record (Joiner et al. 2013). The SIF data from the ESA GOME-2 sensor are available as composited monthly means at a 0.5 degree spatial resolution geographic projection format. The SIF data were re-projected to the 9-km resolution global EASE-grid (V.2) format of the L4_C product using nearest-neighbor resampling. The distributions of GPP and SIF spatial means and ±1 SD spatial variations were computed along 0.05 degree latitudinal bins and compared for relative consistency between the L4_C and GOME-2 datasets. SIF is proportional to canopy absorbed photosynthetically active radiation (APAR) and photosynthesis, but the relationship between SIF (mW m^{-2} sr^{-1} nm^{-1}) and

GPP (g C m^{-2} d^{-1}) can vary according to vegetation type and environmental conditions (Porcar-Castell et al. 2014). Therefore, the SIF and GPP results are presented side-by-side in **Figure 7.11** to allow a qualitative assessment of the inferred productivity patterns.

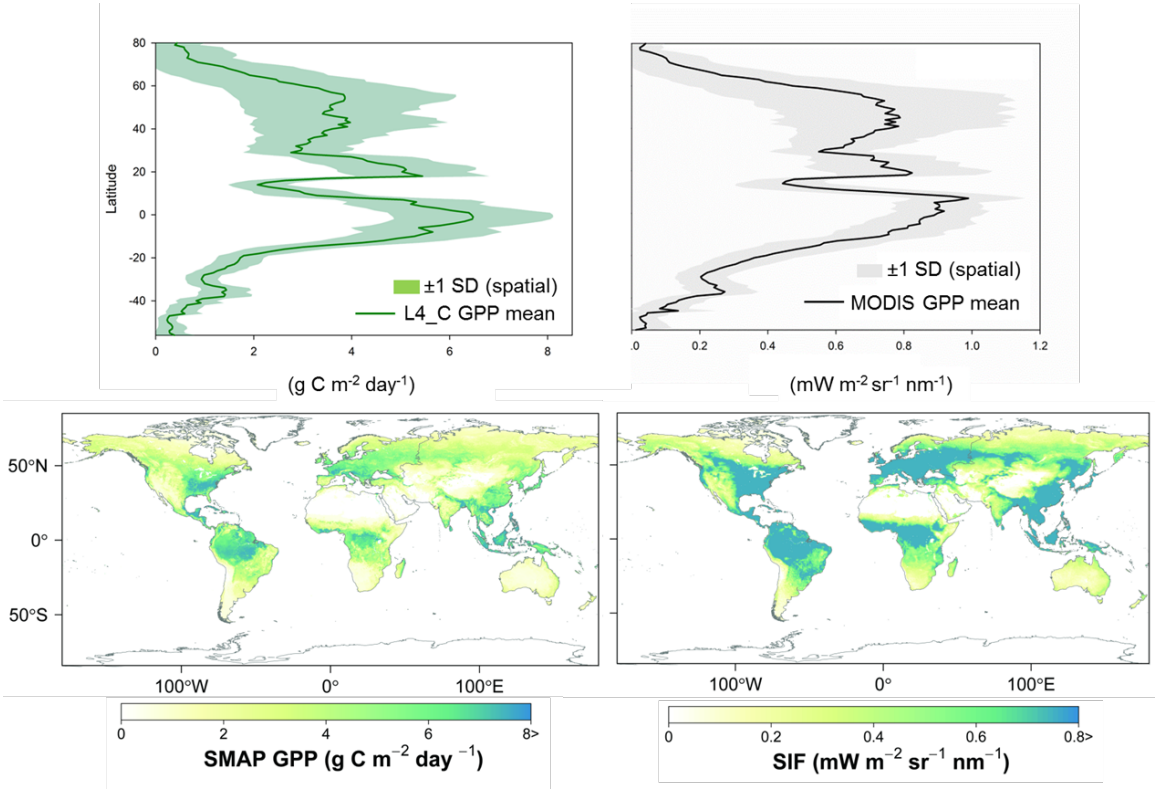

Figure 7.11. Comparison of mean daily GPP outputs (April to July; g C m^{-2} d^{-1}) from the SMAP L4_C product against mean SIF (mW m^{-2} sr^{-1} nm^{-1}) observations from GOME-2 for the same months. Here SIF is used as a proxy for GPP even though the relationship between GPP and SIF can vary, particularly under environmental stress. The L4_C outputs are derived from the initial data record for 2015, while the SIF results represent climatological means derived from a long-term (2007-2013) monthly record. The distributions of GPP and SIF spatial means and ±1 SD spatial variations are summarized within 0.05 degree latitudinal bins (top), while the corresponding mean GPP and SIF global maps are also shown (bottom). White areas in the maps represent barren land, permanent ice, open water bodies and other areas outside of the L4_C product domain.

Both the GOME-2 SIF and L4_C GPP records indicate similar global productivity distributions, including higher productivity rates in the tropical and temperate zones and lower productivity levels at higher latitudes. The spatial productivity patterns are also similar between the two datasets, including generally higher productivity levels over tropical and temperate forests and cropland areas, and lower productivity rates in drier climate zones. There are also, however, notable differences between the two products. The SIF data indicate generally higher productivity rates over croplands, which may be due to incorrect model parameterization and underestimation of optimal light use efficiency levels for intensively managed cropland vegetation (Guanter et al. 2013, Madani et al. 2014). Similar underestimation of cropland productivity levels is also apparent in the MOD17 and MPI-MTE GPP records (e.g. **Figures 7.9 and 7.10**). The L4_C GPP results also indicate relatively lower productivity levels over temperate and tropical forests. Other differences in the productivity patterns are partially attributed to the coarser spatial footprint and temporal compositing of the GOME-2 observations relative to the finer (1-9 km) resolution of the L4_C processing, and differences between the shorter 2015 L4_C sampling period relative to average conditions defined from the long-term (2007-2013) GOME-2 record.

7.4.4 Soil Inventory Records

The L4_C SOC stock estimates from the initial April 2015 record were compared against available static SOC inventory records extending over global (IGBP-DIS) and northern (NCSCD) domains. The L4_C SOC fields are computed on a daily basis as the residual difference between estimated litterfall inputs from vegetation net primary production, and soil heterotrophic respiration losses from the decomposition of soil organic matter. The L4_C SOC estimates are approximately representative of upper soil (<10 cm depth) conditions determined from the surface soil moisture (Wmult) and temperature (Tmult) constraints to the R_h calculations (Kimball et al. 2012). Therefore, surface SOC stocks were estimated from the IGBP and NCSCD global inventory data as a fixed proportion (33.33%) of the reported total soil profile (0-100 cm depth) SOC stock records, though the actual proportion can vary from approximately 29 to 57 percent or more (Jobbagy et al. 2000). These data were then compared against the initial L4_C SOC product outputs from April, 2015. The IGBP and NCSCD maps were re-projected from a 0.5 degree spatial resolution and geographic projection to the 9-km resolution global EASE-grid (V.2) format of the L4_C product using nearest-neighbor resampling. A global SOC difference map was then computed by grid cell-wise subtraction of the estimated IGBP surface SOC values from collocated L4_C SOC values. The distributions of the SOC spatial means and ±1 SD spatial variations were also computed along 0.05 degree latitudinal bins and compared for relative consistency between the inventory records and L4_C data. The NCSCD record is only available for the northern land areas, while the IGBP record extends over the global domain.

The resulting L4_C and IGBP global SOC difference map and the mean latitudinal distributions of the different SOC estimates are presented in **Figure 7.12**. The latitudinal SOC distribution indicated by the L4_C record is similar to the soil inventory records, though the L4_C results are generally at the lower range of the reported inventory data. The L4_C results show a similar increase in SOC levels at higher latitudes consistent with characteristic soil carbon storage increases in colder boreal and tundra soils. The difference map between the L4_C and IGBP results indicates larger model underestimation in northern boreal forest and tundra areas known to contain a large portion of the global soil carbon stock stored in permafrost soils, which have accumulated carbon at relatively slow rates over millennia. The apparent L4_C SOC underestimation in these areas may be due to the recent (2000-2013) NRv4 daily climate record used for model SOC initialization; the observed SOC stocks reflect long-term climate conditions.

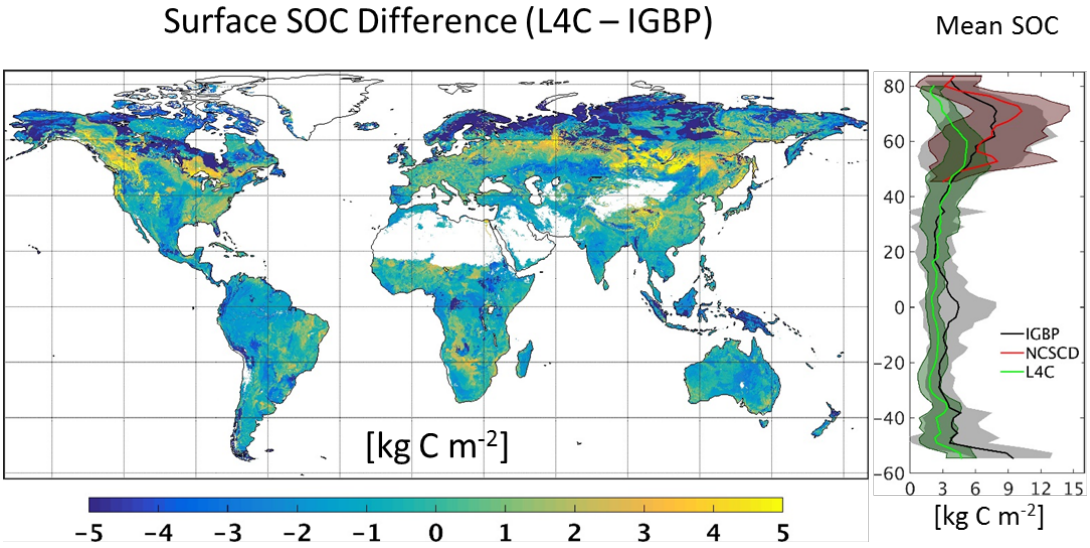

Figure 7.12. Difference map between L4_C and IGBP estimated surface SOC stocks (kg C m^{-2}). The mean latitudinal SOC distributions and ±1 SD spatial variations (shaded) from the L4_C, IGBP and NCSCD records are also shown.

The L4_C results and IGBP inventory record both show generally lower soil carbon stocks in the temperate and tropical zones, though the L4_C results show lower SOC levels than the IGBP record in the tropics, including the African Congo and portions of tropical Southeast Asia. These relatively low L4_C SOC estimates are due to high estimated soil decomposition and Rh rates in warm, moist tropical climate conditions, with minimal constraints from low soil moisture conditions (e.g. **Figure 7.2**). The apparent SOC differences may also reflect regional bias in the GEOS-5 land model-derived daily climate inputs used in the L4_C calculations (Yi et al. 2011).

7.5 Summary

This report provides an assessment and documentation of the SMAP Level 4 Carbon (L4_C) beta product. Methods used to ascertain L4_C beta-product quality and performance included: 1) qualitative evaluations of the product fields for representing expected characteristic spatial and seasonal patterns; 2) comparisons of daily product outputs with tower eddy covariance measurement-based daily carbon (CO_2) flux observations from up to 30 core (CVS) tower sites; 3) comparisons of L4_C daily carbon flux estimates against a larger set of historical tower observations from 228 globally distributed FLUXNET sites; and 4) consistency checks of L4_C product fields against other synergistic global carbon products. This L4_C beta release assessment meets or exceeds CEOS Stage 1 validation criteria based on a limited set of core validation sites. The activities described in this report also satisfy criteria for Stage 2 validation by expanding to regional and global assessments that involve a diverse set of independent observations.

The primary methods and metrics used for the L4_C Cal/Val assessment included comparisons of collocated time series of *in situ* tower observations and L4_C daily outputs. Comparisons involving CVS sites are both spatially and temporally consistent, while comparisons using the more extensive FLUXNET tower site records are spatially but not temporally consistent as they involve product evaluations against historical tower observations. Other methods employed for the evaluations included qualitative comparisons of latitudinal means and spatial patterns between L4_C outputs and other satellite, inventory and model-based products, including the NASA EOS MODIS MOD17 GPP record, the MPI-MTE global tower observation upscaled GPP record, solar-induced canopy fluorescence (SIF) observations from the ESA GOME-2 satellite, and surface soil organic carbon (SOC) stock estimates from global soil inventory records.

Based on these initial assessments, the beta-release L4_C product demonstrates a level of performance and accuracy consistent with the algorithm and product design specifications. The L4_C beta product shows expected characteristic global patterns and seasonality in estimated carbon fluxes and SOC stocks, with no evidence of obvious artifacts or errors in algorithm performance or formatting. The initial L4_C global performance assessment indicates that the beta product meets targeted accuracy requirements for NEE (RMSE$\leq$30 g C m^{-2} y^{-1} or 1.6 g C m^{-2} d^{-1}) over approximately 66% and 83% of global and northern domains, respectively; these results are consistent with the initial CVS and global sparse network tower comparisons. The major L4_C product fields are also generally consistent with similar variables obtained from a diverse set of global benchmark environmental data records. The L4_C beta release is suitable for public distribution and utilization by the larger science and application communities. This beta release also presents an opportunity to enable users to gain familiarity with the parameters and data formats of the product prior to release of the L4_C validated product. The L4_C product performance and accuracy is expected to improve with continuing operations, Cal/Val refinements and reprocessing updates in preparation for the validated product release.

8 OUTLOOK AND PLAN FOR VALIDATED RELEASE

For the beta release the L4_C team Stage 1 and Stage 2 (global assessment) activities have been established and are relatively mature. These Cal/Val program activities will continue toward validated release, including analyses of longer data records and updates from planned calibration refinements. These activities will continue through all Cal/Val stages over the SMAP mission life span. This report notes several limitations in the beta-release version of the L4_C product, including the use of GEOS-5 surface temperatures rather than SMAP microwave sensor-defined freeze-thaw (FT) constraints on the estimated carbon fluxes. These limitations will be addressed prior to the L4_C validated release. The validated release will also include refinements gained from more extensive validation activities involving a longer operational data record and associated calibration improvements to lower order (L3 and L4) inputs to the L4_C algorithms. The validated release will include additional algorithm and product refinements gained from more extensive model sensitivity and validation studies involving several intensive field experiments. These activities will also enable a more comprehensive analysis and quantification of product bias, including systematic and random error components, spatial and seasonal patterns, and error sources. Some issues that should be considered between the beta and validated release include the following:

- *Moving toward a Stage 2+ validated product.* The L4_C beta release is limited by a relatively short (April – July, 2015) period of record assessment. By the time of the planned validated product release in Summer 2016, there will be more than a year of SMAP observations spanning a complete global annual cycle. With enhanced inter-comparisons described below, the L4_C validation level should exceed CEOS validation Stage 2 and be within Stage 3 criteria.
- *Utilization of SMAP FT inputs.* The L4_C beta release defines daily frozen temperature controls to ecosystem productivity using relatively coarse resolution GEOS-5 land model-based surface temperatures. This potentially limits the ability of the L4_C product to address SMAP carbon science objectives to quantify frozen temperature constraints to productivity and improve understanding of the boreal carbon sink. The L4_C validated release will include SMAP microwave sensor-based freeze-thaw (FT) constraints to GPP, with enhanced L-band sensitivity to landscape FT dynamics. These activities will include the utilization of more refined SMAP FT global product inputs with stable performance and demonstrated accuracy. The L4_C validated release should therefore enable a more comprehensive assessment and attainment of the SMAP carbon cycle science objectives.
- *More comprehensive algorithm sensitivity studies.* Detailed L4_C algorithm sensitivity studies will be conducted to evaluate the global impact of SMAP observations on the model-estimated carbon fluxes. These simulations will be conducted by evaluating alternative model simulations derived with and without SMAP observation-informed inputs, including FT and SM inputs and their individual and combined impacts. These simulations will clarify the improved assessment and understanding gained through the SMAP observations on the estimated L4_C product variables spanning a global domain and complete annual cycle. These simulations will also utilize lower order (L3 and L4) SMAP inputs that are relatively mature (post beta release) enabling a more robust assessment of SMAP science impacts.
- *Refined CVS assessment*. The methodology and outcome of the CVS comparisons should be relatively mature by the L4_C validated product stage. Milestones to be completed include acquiring and analyzing a longer set of tower observations spanning a full annual cycle for all participating CVS towers. The tower observation uncertainty is expected to be better characterized and incorporated into the L4_C validation assessment. The CVS matchup software used for the comparisons is also expected to be mature, including the utilization of temporally dynamic data quality metrics for both tower and product outputs.

- *More extensive satellite data comparisons.* A variety of global carbon products have been used for evaluating the general quality and performance of the L4_C beta release. These activities will also be incorporated into the validated assessment but will involve a longer data record spanning a full annual cycle. Additional satellite environmental data records will also be evaluated, including overlapping SIF observations from the NASA Orbiting Carbon Observatory (OCO-2).
- *Incorporating Field Campaign datasets for algorithm assessment and refinement.* Several field campaigns will be completed in 2015, including the Australian SMAPEx and Arizona SMAPVEX15 campaigns. Other airborne field campaigns have recently been completed (e.g., the NASA AirMOSS and CARVE campaigns) that provide extensive ecological data records suitable for L4_C product evaluations. These data will be analyzed in the context of detailed L4_C algorithm sensitivity assessments and product comparisons in preparation for the validated release. These comparisons will focus on spatial scaling assessments, model sensitivity analyses, and performance evaluations involving a large global range of climate and vegetation conditions.

9 ACKNOWLEDGEMENTS

This work used eddy covariance data acquired by the FLUXNET community, which was supported by the CarboEuropeIP, CSIRO, FAO-GTOS-TCO, iLEAPS, Max Planck Institute for Biogeochemistry, National Science Foundation, National Research Insfrastructure for Australia, Terrestrial Ecosystem Research Network, University of Tuscia, Université Laval and Environment Canada, US Department of Energy and NOAA ESRL, as well as many local funders including the Global Change Research Centre AS Czech Republic, Wisconsin Focus on Energy, and Forest Department of the Autonomous Province of Bolzano – CO_2-measuring station of Renon/Ritten. We thank Drs. A.E. Andrews, M. Aurela, D. Baldocchi, J. Beringer, P. Bolstad, J. Cleverly, B.D. Cook, K.J. Davis, A.R. Desai, D. Eamus, E. Euskirchen, J. Goodrich, L. Hutley, A. Kalhori, H. Kwon, B. Law, C. Macfarlane, W. Oechel, S. Prober, K. Rautiainen, R. Scott, H. Wheater, D. Zona and many other PIs for sharing their flux tower data. This document resulted from many hours of diligent analyses and constructive discussion among the L4_C Team, Cal/Val Partners, and other members of the SMAP Project Team. The authors of this report would like to express their gratitude for contributions by the following individuals, who collectively make this document an important milestone for the SMAP project (alphabetically): Joseph Ardizzone, Andreas Colliander, Jinyang Du, Youngwook Kim, Jennifer Watts, Yonghong Yi.

10 REFERENCES

Baccini, A., S.J. Goetz, W.S. Walker, et al., 2012. Estimated carbon dioxide emissions from tropical deforestation improved by carbon-density maps. *Nature Climate Change* 2, 182-185.

Baldocchi, D., 2008: Breathing of the terrestrial biosphere: lessons learned from a global network of carbon dioxide flux measurement systems. *Austr. J. Bot.*, 56: 1-26.

Du, J., J.S. Kimball, M. Azarderakhsh, R.S. Dunbar, M. Moghaddam, and K.C. McDonald, 2015. Classification of Alaska spring thaw characteristics using satellite L-band Radar remote sensing. *IEEE Transactions on Geoscience and Remote Sensing* 53 (1), 542-556.

Entekhabi, D., E.G. Njoku, P.E. O'Neill, et al., 2010. The Soil Moisture Active and Passive (SMAP) Mission. *Proceedings of the IEEE* 98 (5), 704-716.

Entekhabi, D., S. Yueh, P. O'Neill, K. Kellogg et al., SMAP Handbook, JPL Publication, JPL 400-1567, Jet Propulsion Laboratory, Pasadena, California, 182 pages, 2014. https://smap.jpl.nasa.gov/files/smap2/SMAP_Handbook_FINAL_1_JULY_2014_Web.pdf.

Glassy, J., J.S. Kimball, R.H. Reichle, J.V. Ardizzone, G-K. Kim, R.A. Lucchesi, and B.H. Weiss, 2015. Soil Moisture Active Passive (SMAP) Mission Level 4 Carbon (L4_C) Product Specification Document. GMAO Office Note No. 12 (Version 1.9), 71 pp, NASA Goddard Space Flight Center, Greenbelt, MD, USA. Available from http://gmao.gsfc.nasa.gov/pubs/office_notes.

Guanter, L., Y. Zhang, M. Jung, et al. 2013. Global and time-resolved monitoring of crop photosynthesis with chlorophyll fluorescence. *PNAS* 111, 14, E1327-E1333.

Global Soil Data Task Group. 2000. Global Gridded Surfaces of Selected Soil Characteristics (IGBP-DIS). [Global Gridded Surfaces of Selected Soil Characteristics (International Geosphere-Biosphere Programme - Data and Information System)]. Data set. Available on-line [http://www.daac.ornl.gov] from Oak Ridge National Laboratory Distributed Active Archive Center, Oak Ridge, Tennessee, U.S.A. doi:10.3334/ORNLDAAC/569.

Hugelius, G., J. Strauss, S. Zubrzycki, et al., 2014. Estimated stocks of circumpolar permafrost carbon with quantified uncertainty ranges and identified data gaps. *Biogeosciences* 11, 6573-6593.

Jackson, T., A. Colliander, J. Kimball, R. Reichle, W. Crow, D. Entekhabi, P. O'Neill, and E. Njoku, 2014. SMAP Science Data Calibration and Validation Plan. SMAP Project, JPL D-52544, Jet Propulsion Laboratory, Pasadena CA, 96 pp (http://smap.jpl.nasa.gov/files/smap2/CalVal_Plan_120706_pub.pdf).

Jobbagy, E. G., & R. B. Jackson. 2000. The vertical distribution of soil organic carbon and its relation to climate and vegetation. *Ecol. Applications*, 10 (2): pp. 423-36.

Joiner, J., L. Gaunter, R. Lindstrot, et al., 2013. Global monitoring of terrestrial chlorophyll fluorescence from moderate-spectral-resolution near-infrared satellite measurements: methodology, simulations, and application to GOME-2. *Atmos. Meas. Tech*., 6, 2803-2823.

Jung, M., M. Reichstein, H.A. Margolis, et al., 2010. Global patterns of land-atmosphere fluxes of carbon dioxide, latent heat, and sensible heat derived from eddy covariance, satellite, and meteorological observations. *J. Geophys. Res. Biogeosci*. 116, G3, DOI:10.1029/2010JG001566.

Kimball, J.S., L.A. Jones, J.P. Glassy, and R. Reichle, 2014. SMAP Algorithm Theoretical Basis Document, Release A: L4 Carbon Product. SMAP Project, JPL D-66484, Jet Propulsion Laboratory, Pasadena CA., 76 pp, (http://smap-archive.jpl.nasa.gov/files/smap2/L4_C_RevA.pdf).

Madani, N., J.S. Kimball, D.L.R. Affleck, J. Kattge, J. Graham, P.M. van Bodegom, P.B. Reich, and S.W. Running, 2014. Improving ecosystem productivity modeling through spatially explicit estimation of optimal light use efficiency. *J. Geophys. Res. Biogeosci*., 119, 9, 1755-1769.

Porcar-Castell, A., E. Tyystjarvi, J. Atherton, et al., 2014. Linking chlorophyll a fluorescence to photosynthesis for remote-sensing applications: mechanisms and challenges. *Journal of Experimental Botany* 66, 19, doi:101093/jxb/eru191.

Schimel, D., R. Pavlick, J.B. Fisher, et al. 2015. Observing terrestrial ecosystems and the carbon cycle from space. *Global Change Biology* 21, 1762-1776.

Turner, D.P., W.D. Ritts, W.B. Cohen, et al. 2006. Evaluation of MODIS NPP and GPP products across multiple biomes. *Remote Sensing of Environment*, 102, 3-4, 282-292.

Yi, Y., J.S. Kimball, L.A. Jones, R.H. Reichle and K.C. McDonald, 2011. Evaluation of MERRA land surface estimates in preparation for the Soil Moisture Active Passive Mission. *Journal of Climate* 24(15), 3797-3816.

Yi, Y., J.S. Kimball, L.A. Jones, R.H. Reichle, R. Nemani, and H.A. Margolis, 2013. Recent climate and fire disturbance impacts on boreal and arctic ecosystem productivity estimated using a satellite-based terrestrial carbon flux model. *J. Geophys. Res*. *Biogeosci*. 118, 1-17.

Zhao, M., and S.W. Running, 2010. Drought-induced reduction in global terrestrial net primary production from 2000 through 2009. *Science* 329, 5994, 940-943.

Previous Volumes in This Series

Volume 1 *September 1994*	Documentation of the Goddard Earth Observing System (GEOS) general circulation model - Version 1 **L.L. Takacs, A. Molod, and T. Wang**
Volume 2 *October 1994*	Direct solution of the implicit formulation of fourth order horizontal diffusion for gridpoint models on the sphere **Y. Li, S. Moorthi, and J.R. Bates**
Volume 3 *December 1994*	An efficient thermal infrared radiation parameterization for use in general circulation models **M.-D. Chou and M.J. Suarez**
Volume 4 *January 1995*	Documentation of the Goddard Earth Observing System (GEOS) Data Assimilation System - Version 1 **James Pfaendtner, Stephen Bloom, David Lamich, Michael Seablom, Meta Sienkiewicz, James Stobie, and Arlindo da Silva**
Volume 5 *April 1995*	Documentation of the Aries-GEOS dynamical core: Version 2 **Max J. Suarez and Lawrence L. Takacs**
Volume 6 *April 1995*	A Multiyear Assimilation with the GEOS-1 System: Overview and Results **Siegfried Schubert, Chung-Kyu Park, Chung-Yu Wu, Wayne Higgins, Yelena Kondratyeva, Andrea Molod, Lawrence Takacs, Michael Seablom, and Richard Rood**
Volume 7 *September 1995*	Proceedings of the Workshop on the GEOS-1 Five-Year Assimilation **Siegfried D. Schubert and Richard B. Rood**
Volume 8 *March 1996*	Documentation of the Tangent Linear Model and Its Adjoint of the Adiabatic Version of the NASA GEOS-1 C-Grid GCM: Version 5.2 **Weiyu Yang and I. Michael Navon**
Volume 9 *March 1996*	Energy and Water Balance Calculations in the Mosaic LSM **Randal D. Koster and Max J. Suarez**
Volume 10 *April 1996*	Dynamical Aspects of Climate Simulations Using the GEOS General Circulation Model **Lawrence L. Takacs and Max J. Suarez**

Volume 11 *May 1997*	Documentation of the Tangent Linear and its Adjoint Models of the Relaxed Arakawa-Schubert Moisture Parameterization Package of the NASA GEOS-1 GCM (Version 5.2) **Weiyu Yang, I. Michael Navon, and Ricardo Todling**
Volume 12 *August 1997*	Comparison of Satellite Global Rainfall Algorithms **Alfred T.C. Chang and Long S. Chiu**
Volume 13 *December 1997*	Interannual Variability and Potential Predictability in Reanalysis Products **Wie Ming and Siegfried D. Schubert**
Volume 14 *August 1998*	A Comparison of GEOS Assimilated Data with FIFE Observations **Michael G. Bosilovich and Siegfried D. Schubert**
Volume 15 *June 1999*	A Solar Radiation Parameterization for Atmospheric Studies **Ming-Dah Chou and Max J. Suarez**
Volume 16 *November 1999*	Filtering Techniques on a Stretched Grid General Circulation Model **Lawrence Takacs, William Sawyer, Max J. Suarez, and Michael S. Fox-Rabinowitz**
Volume 17 *July 2000*	Atlas of Seasonal Means Simulated by the NSIPP-1 Atmospheric GCM **Julio T. Bacmeister, Philip J. Pegion, Siegfried D. Schubert, and Max J. Suarez**
Volume 18 *December 2000*	An Assessment of the Predictability of Northern Winter Seasonal Means with the NSIPP1 AGCM **Philip J. Pegion, Siegfried D. Schubert, and Max J. Suarez**
Volume 19 *July 2001*	A Thermal Infrared Radiation Parameterization for Atmospheric Studies **Ming-Dah Chou, Max J. Suarez, Xin-Zhong, and Michael M.-H. Yan**
Volume 20 *August 2001*	The Climate of the FVCCM-3 Model **Yehui Chang, Siegfried D. Schubert, Shian-Jiann Lin, Sharon Nebuda, and Bo-Wen Shen**
Volume 21 *September 2001*	Design and Implementation of a Parallel Multivariate Ensemble Kalman Filter for the Poseidon Ocean General Circulation Model **Christian L. Keppenne and Michele M. Rienecker**
Volume 22 *August 2002*	Coupled Ocean-Atmosphere Radiative Model for Global Ocean Biogeochemical Models **Watson W. Gregg**

Volume 23 *November 2002*	Prospects for Improved Forecasts of Weather and Short-term Climate Variability on Subseasonal (2-Week to 2-Month) Time Scales **Siegfried D. Schubert, Randall Dole, Huang van den Dool, Max J. Suarez, and Duane Waliser**
Volume 24 *July 2003*	Temperature Data Assimilation with Salinity Corrections: Validation for the NSIPP Ocean Data Assimilation System in the Tropical Pacific Ocean, 1993–1998 **Alberto Troccoli, Michele M. Rienecker, Christian L. Keppenne, and Gregory C. Johnson**
Volume 25 *December 2003*	Modeling, Simulation, and Forecasting of Subseasonal Variability **Duane Waliser, Siegfried D. Schubert, Arun Kumar, Klaus Weickmann, and Randall Dole**
Volume 26 *April 2005*	Documentation and Validation of the Goddard Earth Observing System (GEOS) Data Assimilation System – Version 4 **Senior Authors: S. Bloom, A. da Silva and D. Dee** **Contributing Authors: M. Bosilovich, J-D. Chern, S. Pawson, S. Schubert, M. Sienkiewicz, I. Stajner, W-W. Tan, and M-L. Wu**
Volume 27 *December 2008*	The GEOS-5 Data Assimilation System - Documentation of Versions 5.0.1, 5.1.0, and 5.2.0. **M.M. Rienecker, M.J. Suarez, R. Todling, J. Bacmeister, L. Takacs, H.-C. Liu, W. Gu, M. Sienkiewicz, R.D. Koster, R. Gelaro, I. Stajner, and J.E. Nielsen**
Volume 28 *April 2012*	The GEOS-5 Atmospheric General Circulation Model: Mean Climate and Development from MERRA to Fortuna **Andrea Molod, Lawrence Takacs, Max Suarez, Julio Bacmeister, In-Sun Song, and Andrew Eichmann**
Volume 29 *May 2012*	Atmospheric Reanalyses – Recent Progress and Prospects for the Future. A Report from a Technical Workshop, April 2010 **Michele M. Rienecker, Dick Dee, Jack Woollen, Gilbert P. Compo, Kazutoshi Onogi, Ron Gelaro, Michael G. Bosilovich, Arlindo da Silva, Steven Pawson, Siegfried Schubert, Max Suarez, Dale Barker, Hirotaka Kamahori, Robert Kistler, and Suranjana Saha**
Volume 30 *September 2012*	The GEOS-ODAS, description and evaluation **Guillaume Vernieres, Michele M. Rienecker, Robin Kovach and Christian L. Keppenne**

Volume 31 *March 2013*	Global Surface Ocean Carbon Estimates in a Model Forced by MERRA **Watson W. Gregg, Nancy W. Casey and Cecile S. Rousseaux**
Volume 32 **March 2014**	Estimates of AOD Trends (2002-2012) over the World's Major Cities based on the MERRA Aerosol Reanalysis **Simon Provencal, Pavel Kishcha, Emily Elhacham, Arlindo M. da Silva, and Pinhas Alpert**
Volume 33 **August 2014**	The Effects of Chlorophyll Assimilation on Carbon Fluxes in a Global Biogeochemical Model **Cécile S. Rousseaux and Watson W. Gregg**
Volume 34 **September 2014**	Background Error Covariance Estimation using Information from a Single Model Trajectory with Application to Ocean Data Assimilation into the GEOS-5 Coupled Model **Christian L. Keppenne, Michele M. Rienecker, Robin M. Kovach, and Guillaume Vernieres**
Volume 35 **December 2014**	Observation-Corrected Precipitation Estimates in GEOS-5 **Rolf H. Reichle and Qing Liu**
Volume 36 **March 2015**	Evaluation of the 7-km GEOS-5 Nature Run **Ronald Gelaro, William M. Putman, Steven Pawson, Clara Draper, Andrea Molod, Peter M. Norris, Lesley Ott, Nikki Prive, Oreste Reale, Deepthi Achuthavarier, Michael Bosilovich, Virginie Buchard, Winston Chao, Lawrence Coy, Richard Cullather, Arlindo da Silva, Anton Darmenov, Ronald M. Errico, Marangelly Fuentes, Min-Jeong Kim, Randal Koster, Will McCarty, Jyothi Nattala, Gary Partyka, Siegfried Schubert, Guillaume Vernieres, Yuri Vikhliaev, and Krzysztof Wargan**
Volume 37 **March 2015**	Maintaining Atmospheric Mass and Water Balance within Reanalysis **Lawrence L. Takacs, Max Suarez, and Ricardo Todling**

Volume 38 *September 2015*	The Quick Fire Emissions Dataset (QFED) – Documentation of versions 2.1, 2.2 and 2.4 **Anton S. Darmenov and Arlindo da Silva**
Volume 39 *September 2015*	Land Boundary Conditions for the Goddard Earth Observing System Model Version 5 (GEOS-5) Climate Modeling System – Recent Updates and Data File Descriptions **Sarith P. Mahanama, Randal D. Koster, Gregory K. Walker, Lawrence L. Takacs, Rolf H. Reichle, Gabrielle De Lannoy, Qing Liu, Bin Zhao, and Max J. Suarez**
Volume 40 *October 2015*	Soil Moisture Active Passive (SMAP) Project Assessment Report for the Beta-Release L4_SM Data Product **Rolf H. Reichle, Gabrielle J. M. De Lannoy, Qing Liu, Andreas Colliander, Austin Conaty, Thomas Jackson, John Kimball, and Randal D. Koster**
Volume 41 *October 2015*	GDIS Workshop Report **Siegfried Schubert, Will Pozzi , Eric F. Wood , Kerstin Stahl , Mike Hayes, Juergen Vogt, Sonia Seneviratne, Ron Stewart, Roger Pulwarty, Robert Stefanski**